Interface dynamics of a metastable mass-conserving spatially extended diffusion

Nils Berglund, Sébastien Dutercq

Abstract

We study the metastable dynamics of a discretised version of the mass-conserving stochastic Allen–Cahn equation. Consider a periodic one-dimensional lattice with N sites, and attach to each site a real-valued variable, which can be interpreted as a spin, as the concentration of one type of metal in an alloy, or as a particle density. Each of these variables is subjected to a local force deriving from a symmetric double-well potential, to a weak ferromagnetic coupling with its nearest neighbours, and to independent white noise. In addition, the dynamics is constrained to have constant total magnetisation or mass. Using tools from the theory of metastable diffusion processes, we show that the long-term dynamics of this system is similar to a Kawasaki-type exchange dynamics, and determine explicit expressions for its transition probabilities. This allows us to describe the system in terms of the dynamics of its interfaces, and to compute an Eyring–Kramers formula for its spectral gap. In particular, we obtain that the spectral gap scales like the inverse system size squared.

Date. August 18, 2015.

2010 *Mathematical Subject Classification.* 60J60, 60K35 (primary), 82C21, 82C24 (secondary)

Keywords and phrases. Metastability, Kramers' law, stochastic exit problem, Allen–Cahn equation, Kawasaki dynamics, interface, spectral gap.

1 Introduction

The low-temperature dynamics of spatially extended systems often displays metastability: these systems can spend considerable amounts of time in configurations that have higher energy than their ground state. Well-known examples of such phenomena are supercooled water, which remains liquid at temperatures below 0°C, a supersaturated gas, which does not condensate although this would be thermodynamically more favourable, and a wrongly magnetised ferromagnet.

Much research effort has been dedicated to the study of metastable lattice systems, such as the Ising model at low temperature. This has led to very precise results on the time the system spends in metastable equilibrium, on the way it moves from a metastable to a stable state by creating a critical droplet, and on the shape of this droplet. See for instance [14] for a review on Ising models with Glauber (spin flip) dynamics and lattice gases with Kawasaki (particle/hole exchange) dynamics, and [27] for results based on the theory of large deviations. A considerably more difficult case arises when there is no underlying lattice given a priori, but particles instead evolve in $\mathbb{R}^d$, and one wants to describe processes such as crystallisation. For recent results in this direction, see for instance [23, 19, 15].

Another type of models whose metastable behaviour is understood in detail are diffusion processes described by stochastic differential equations with weak noise. A general large-deviation approach to these equations goes back to the work of Freidlin and Wentzell [20],

which provides many results on transition times between attractors and on the long-time dynamics. In the case of reversible diffusions (that is, those satisfying a detailed balance condition), metastable timescales are governed by the so-called Eyring–Kramers formula, derived heuristically in [18, 25], and first proved in a mathematically rigorous way in [10, 11]. See for instance [4] for a recent survey on various methods of proof and extensions of the result.

A spatially extended system of coupled diffusions, which can be considered of intermediate difficulty between lattice systems with discrete spins and systems of particles evolving in $\mathbb{R}^d$, was introduced in [6, 7]. In this model, the spins are still attached to a lattice (which is periodic and one-dimensional of size N), but they take values in $\mathbb{R}$ instead of $\{-1, +1\}$. Each spin feels a local symmetric double-well potential with minima in ± 1, and is coupled ferromagnetically to its nearest neighbours. In addition, each spin is subjected to independent white noise. For weak coupling, the dynamics of this system was shown to be similar to that of an Ising model with Glauber spin-flip dynamics. Indeed, the energy of configurations increases with the number of *interfaces*, defined as pairs of neighbouring spins having different sign. As a consequence, the system favours configurations with few clusters of spins having the same sign. On the other hand, when the coupling scales like N^2, the system converges as $N \to \infty$ to an Allen–Cahn SPDE with space-time white noise, whose metastable behaviour was studied in [9, 2].

A natural question that arises is whether one can construct a similar system, with continuous spins attached to a discrete lattice, but whose dynamics for weak coupling resembles Kawasaki exchange dynamics instead of Glauber spin-flip dynamics. In other words, one would like to impose that the total magnetisation (or the total mass in lattice gas terminology) is conserved. A simple way of doing this is to start with the potential energy of the system considered in [6, 7], and to constrain it to the hypersurface where the sum of all spins is constant, say equal to zero. This is nothing but the discretised version of the mass-conserving Allen–Cahn equation introduced in [29]. The objective of the present work is to study the metastable dynamics of this model.

It is quite easy to see that in the uncoupled limit, the potential energy of the constrained system is minimal when exactly half the sites have value $+1$, while the other half have value -1. Such states have a clear particle system interpretation: just consider each $+1$ as a particle and each -1 as a hole. As in the unconstrained case, for weak positive coupling, the energy of configurations increases with the number of interfaces. Therefore the ground state consists of the configurations having exactly one cluster of particles and one cluster of holes, separated by two interfaces. Higher-energy configurations have more clusters and more interfaces. Thus if the system starts in an excited state with many interfaces, one expects that its clusters will gradually merge, reducing the number of interfaces, until the ground state is reached (Figure 1).

While our analysis will show that this picture is essentially correct, there is a complication due to the fact that particle/hole configurations are *not* the only local minima of the potential energy. Somewhat unexpectedly, there turn out to be many more "spurious" local minima, whose coordinates are not close to ± 1. The way around this difficulty is to realise that all spurious configurations have a higher energy than the particle/hole configurations. Therefore the long-term dynamics will spend most of the time near the particle/hole configurations, with occasional transitions between them. Our main result is the characterisation of this effective dynamics.

This paper is organised as follows. In Section 2, we give a precise definition of the considered model. In Section 3, we describe the potential landscape of the model, meaning

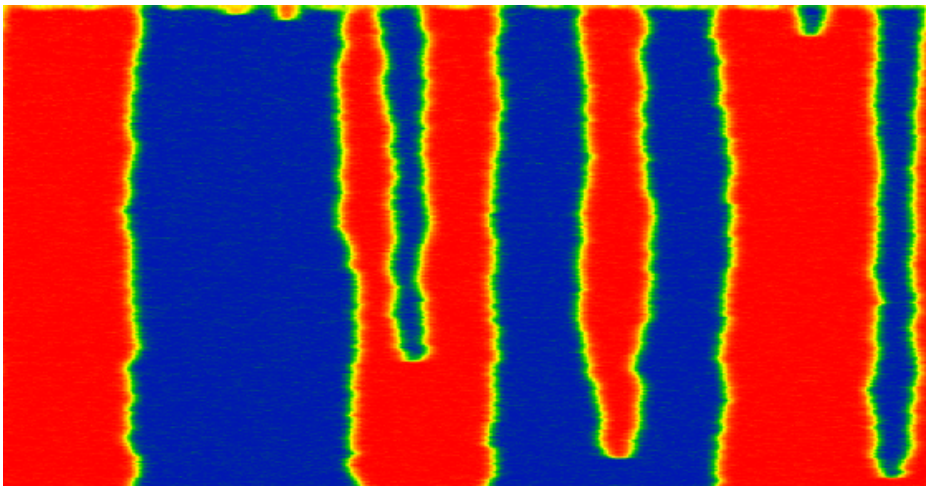

FIGURE 1. Example of evolution of the constrained system (2.7) with $N = 512$ sites. Space goes from left to right, and time from top to bottom. Blue and red correspond to spin values close to -1 and 1 respectively. The system starts in a configuration with 40 interfaces, many of which disappear quickly. At the end of the simulation, the number of interfaces has been reduced to 4. Parameter values are $\varepsilon = 0.02$ and $\gamma = 16$. This coupling intensity, which is much larger than considered in this work, has been chosen to obtain transitions on an observable timescale.

that we find all local minima of the potential energy, and describe how they are connected by saddles with one unstable direction. Section 4 uses the notion of metastable hierarchy to show that the dynamics indeed concentrates on particle/hole configurations, and derives the effective dynamics on these states. In Section 5 we use this information to characterise the evolution of interfaces, and we derive a sharp estimate for the spectral gap of the system, which determines the relaxation time to equilibrium. Section 6 contains concluding remarks, while most proofs are postponed to the appendix.

Notations: If $i \leqslant j$ are integers, $[\![i, j]\!]$ denotes the set $\{i, i+1, \dots, j\}$. The cardinality of a finite set A is denoted by $|A|$, and $A = B \cup C$ indicates that $A = B \cup C$ with B and C disjoint. We write 1_A for the indicator function of the set A, $\mathbb{1}_n$ or simply $\mathbb{1}$ for the identity matrix of size $n \times n$, and $\mathbf{1}$ for a column vector with all components equal to 1. Finally, we write $\mathbb{E}^\mu[\cdot]$ for expectations with respect to the law of the diffusion process started with distribution μ, and $\mathbb{E}^x[\cdot]$ in case μ is concentrated in a single point x.

Acknowledgements: The idea of studying the constrained process considered in this work goes back to a question Erwin Bolthausen asked after a talk given in Zürich by the first author on the unconstrained model studied in [6, 7].

2 Definition of the model

Consider the potential $V_\gamma : \mathbb{R}^N \to \mathbb{R}$ defined by

$$V_\gamma(x) = \sum_{i=1}^{N} U(x_i) + \frac{\gamma}{4} \sum_{i=1}^{N} (x_{i+1} - x_i)^2 \,, \qquad U(\xi) = \frac{1}{4}\xi^4 - \frac{1}{2}\xi^2 \,, \tag{2.1}$$

where $N \geqslant 2$ is an integer and $\gamma \geqslant 0$ is a coupling parameter. We also make the identification $x_{N+1} = x_1$, that is, we consider periodic boundary conditions. Thus x can be considered

either as an element of $\mathbb{R}^N$, or as an element of $\mathbb{R}^\Lambda$, where Λ is the periodic lattice $\mathbb{Z}/N\mathbb{Z}$.

The potential V_γ allows to define a diffusion process by the stochastic differential equation

$$\mathrm{d}x_t = -\nabla V_\gamma(x_t)\,\mathrm{d}t + \sqrt{2\varepsilon}\,\mathrm{d}W_t\,, \tag{2.2}$$

where W_t is an N-dimensional Wiener process, and $\varepsilon \geqslant 0$ is a small parameter measuring noise intensity. The dynamics of this system has already been studied in [6, 7]. Here we are interested in a different system, obtained by constraining the diffusion to the hyperplane

$$S = \left\{ x \in \mathbb{R}^N \colon \sum_{i=1}^N x_i = 0 \right\}. \tag{2.3}$$

To define its dynamics, let R be an orthogonal matrix mapping the unit normal vector to S to the Nth canonical basis vector e_N. Let $\widehat{V}_\gamma(y) = V_\gamma(R^{-1}y)$, and define the dynamics by

$$\begin{aligned} \mathrm{d}y_{i,t} &= -\frac{\partial \widehat{V}_\gamma(y)}{\partial y_{i,t}}\,\mathrm{d}t + \sqrt{2\varepsilon}\,\mathrm{d}W_{i,t}\,, \qquad i = 1, \dots, N-1\,, \\ y_{N,t} &= 0\,, \end{aligned} \tag{2.4}$$

where $W_{1,t}, \dots, W_{N-1,t}$ are independent Brownian motions. Then x_t is by definition the process $x_t = R^{-1}y_t$. It is easy to check that this definition does not depend on the choice of R.

An equivalent way of defining the dynamics is to write

$$\mathrm{d}y_t = \left[-\nabla \widehat{V}_\gamma(y_t) + \langle \nabla \widehat{V}_\gamma(y_t), e_N\rangle e_N\right] + \sqrt{2\varepsilon}\,\mathrm{d}W_t \tag{2.5}$$

where W_t is an $(N-1)$-dimensional Wiener process. Indeed, the extra term precisely ensures that the N-th component of the drift term vanishes. Transforming back, we obtain the equation

$$\mathrm{d}x_t = \left[-\nabla V_\gamma(x_t) + \frac{1}{N}\langle \nabla V_\gamma(x_t), \mathbf{1}\rangle \mathbf{1}\right]\mathrm{d}t + \sqrt{2\varepsilon}\,\mathrm{d}\widetilde{W}_t\,, \tag{2.6}$$

where $\mathbf{1}$ denotes the vector with all components equal to 1 (hence the normalisation $1/N$), and $\widetilde{W}_t = R^{-1}W_t$ is a Brownian motion on S. When written in components, the resulting dynamics takes the form

$$\mathrm{d}x_{i,t} = \left[f(x_{i,t}) + \frac{\gamma}{2}(x_{i+1,t} - 2x_{i,t} + x_{i-1,t}) - \frac{1}{N}\sum_{j=1}^N f(x_{j,t})\right]\mathrm{d}t + \sqrt{2\varepsilon}\,\mathrm{d}\widetilde{W}_{j,t} \tag{2.7}$$

where $f(\xi) = -U'(\xi) = \xi - \xi^3$ (and the $\widetilde{W}_{j,t}$ are no longer independent). Note that this is a discretised version of the mass-conserving Allen–Cahn SPDE

$$\partial_t u(t,x) = \gamma \Delta u(t,x) + f(u(t,x)) - \frac{1}{L}\int_0^L f(u(t,y))\,\mathrm{d}y + \sqrt{2\varepsilon}\,\xi(t,x) \tag{2.8}$$

with space-time white noise ξ on S. The nonlocal integral term indeed ensures that the total mass $\int_0^L u(t,x)\,\mathrm{d}x$ is conserved. This equation was introduced in [29] in the case without noise, and considered recently in [1] in the case with noise.

Systems of the form (2.2) admit a unique invariant probability measure with density

$$\mu(x) = \frac{1}{Z}\,\mathrm{e}^{-V(x)/\varepsilon}\,, \tag{2.9}$$

where Z is the normalisation constant, and are reversible with respect to μ. Analogous statements hold true for the system constructed here (except that μ is concentrated on the hyperplane S). The questions we thus ask are the following:

- How long does the system take to relax to equilibrium?
- What are the typical paths taken to achieve equilibrium, when starting in an atypical configuration?
- Can the system be approximated by a coarse-grained process visiting only local minima of the potential? What does this coarse-grained process look like?

3 Potential landscape

3.1 The transition graph

For a general system of the form (2.2), let

$$\mathcal{S} = \big\{x \in \mathbb{R}^N \colon \nabla V_\gamma(x) = 0\big\} \tag{3.1}$$

be the set of all stationary points of V_γ. A stationary point $x^\star \in \mathcal{S}$ is called *non-degenerate* if its Hessian matrix $\nabla^2 V_\gamma(x^\star)$ has a nonzero determinant. We will assume for simplicity that all stationary points of V_γ are nondegenerate (see however [8] for results on systems with degenerate stationary points).

The *Morse index* of a nondegenerate stationary point $x^\star$ is the number of negative eigenvalues of the Hessian $\nabla^2 V_\gamma(x^\star)$ (i.e., the number of directions in which V_γ decreases near $x^\star$). For each $k \in [\![0, N]\!]$, let $\mathcal{S}_k$ denote the set of stationary points of index k. The set $\mathcal{S}_0$ of local minima of V_γ and the set $\mathcal{S}_1$ of saddles of index 1 (or 1-saddles) are the most important for the stochastic dynamics for small ε.

By the stable manifold theorem, each 1-saddle has a one-dimensional unstable manifold consisting in two connected components. Along each component, the value of V_γ has to decrease, and therefore (since V_γ is confining) both components have to converge to a local minimum of V_γ. Let $\mathcal{G} = (\mathcal{S}_0, \mathcal{E})$ be the unoriented graph in which two elements of $\mathcal{S}_0$ are connected by an edge in $\mathcal{E}$ if and only if there exists a 1-saddle $z \in \mathcal{S}_1$ whose unstable manifold converges to these local minima.

Roughly speaking, the stochastic system behaves for small noise intensity ε like a Markovian jump process (or continuous-time Markov chain) on $\mathcal{S}_0$, with jump rates related to the potential differences between local minima and 1-saddles. This is the basic idea implemented in [20, Chapter 6], and there are many refinements on which we will comment in more detail below.

In the case of the potential (2.1) without constraint, the potential landscape has been analysed in [6]. In particular, the following properties have been obtained:

- If $\gamma = 0$, the set of stationary points is given by $\mathcal{S} = \{-1, 0, 1\}^N$. The local minima are given by $\mathcal{S}_0 = \{-1, 1\}^N$ and the 1-saddles are those stationary points that have exactly one coordinate equal to 0. They connect the local minima obtained by replacing the 0 coordinate by -1 or $+1$. Thus the graph $\mathcal{G}$ is an N-dimensional hypercube, with transitions consisting in the reversal of the sign of one coordinate, which can be interpreted as spin flips.
- There exists a critical coupling $\gamma^*(N)$, satisfying $\gamma^*(N) \geqslant \frac{1}{4}$ for all N, such that the transition graph $\mathcal{G}$ is the same for all $\gamma \in [0, \gamma^*(N))$. Thus the local minima and allowed transitions are the same for weak positive coupling as in the uncoupled case.

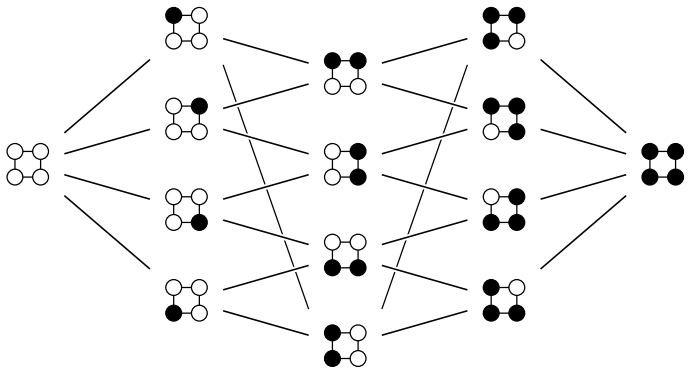

FIGURE 2. Transition graph of the unconstrained system for $N = 4$ and $\gamma = 0$. Black and white circles represent respectively coordinates equal to 1 and to -1. The two configurations $(1, -1, 1, -1)$ and $(-1, 1, -1, 1)$ are not shown, because they correspond to non-optimal transitions as soon as $\gamma > 0$.

What changes, however, is that some transitions are easier than others when $\gamma > 0$: the systems prefers transitions that minimise the number of interfaces, that is, the number of nearest neighbours with a different sign (Figure 2). The stochastic dynamics is thus very close to the one of an Ising model with Glauber spin-flip dynamics.

- For γ increasing beyond $\gamma^*(N)$, the system undergoes a number of bifurcations that reduce the number of stationary points. In particular, for $\gamma > 1/(2\sin^2(\pi/N))$ the system synchronises: there are only two local minima given by $\pm(1, 1, \ldots, 1)$, connected by the only 1-saddle which is at the origin.

Our aim is now to obtain similar results for the graph $\mathcal{G}$ of the constrained system, starting with the uncoupled case $\gamma = 0$ and then moving to small positive γ.

3.2 The uncoupled case

We consider in this section the dynamics of the constrained system in the uncoupled case $\gamma = 0$. The above definitions of $\mathcal{S}_0$, $\mathcal{S}_1$ and $\mathcal{G}$ can be adapted to the constained case, either by considering the $N - 1$ first equations in (2.4), or by solving a constrained optimisation problem. In particular, the stationary points have to satisfy

$$\nabla V_0(x) = \lambda \mathbf{1} \tag{3.2}$$

for a Lagrange multiplier $\lambda \in \mathbb{R}$ (this is indeed consistent with (2.6)). In addition, the constraint $x \in S$ has to be satisfied.

In components, the condition (3.2) becomes

$$x_i^3 - x_i = \lambda \,, \qquad i = 1, \ldots, N \,. \tag{3.3}$$

Let $\lambda_c = \frac{2}{3\sqrt{3}}$. The equation $\xi^3 - \xi = \lambda$ has three real solutions if $|\lambda| < \lambda_c$, two real solutions if $|\lambda| = \lambda_c$ and one real solution otherwise. The last case is incompatible with the constraint $x \in S$, while the second case can only occur if N is a multiple of 3, because then the two solutions of $\xi^3 - \xi = \lambda$ have a $(-2 : 1)$ ratio.

We henceforth assume that $|\lambda| < \lambda_c$, and denote by $\alpha_0, \alpha_1, \alpha_2$ the distinct roots of $\xi^3 - \xi - \lambda$. Then each x_i solving (3.3) has to be equal to one of the α_j. We let a_j be the

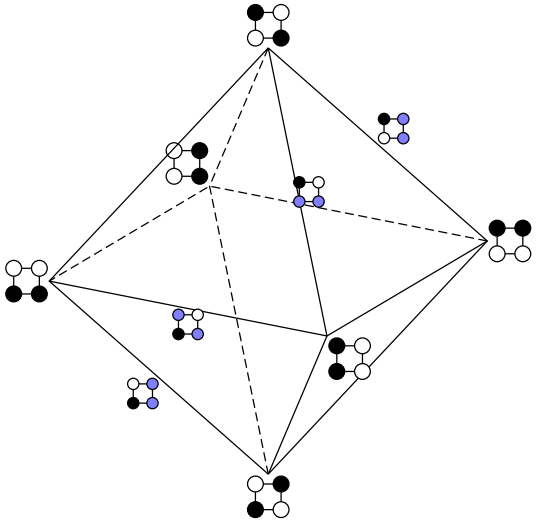

FIGURE 3. Transition graph of the constrained system for $N = 4$ and $\gamma = 0$. Black and white circles represent respectively coordinates equal to 1 and to -1. A few 1-saddles associated with edges of the graph are shown, with blue circles indicating coordinates equal to 0.

number of occurrences of α_j, and reorder the α_j in such a way that $a_0 \leqslant a_1 \leqslant a_2$. We denote such a stationary point by the triple (a_0, a_1, a_2). Observe that we necessarily have $a_0 + a_1 + a_2 = N$.

Proposition 3.1 (Local minima and 1-saddles for $\gamma = 0$)**.** *Assume that N is not a multiple of 3, and let $x^\star$ be a critical point with triple (a_0, a_1, a_2). Then*

- *if $2a_1 > a_0 + a_2$, then $x^\star$ is a stationary point of index a_0;*
- *if $2a_1 < a_0 + a_2$, then $x^\star$ is a stationary point of index $a_2 - 1$.*

We give the proof in Appendix A.1. It is based on the construction of an orthogonal basis around each stationary point, in which the Hessian matrix is block-diagonal with blocks of size 3 at most, so that the signs of its eigenvalues can be determined.

Remark 3.2. The case $2a_1 = a_0 + a_2$ can only occur if N is a multiple of 3, because $a_0 + a_2 = N - a_1$ would imply $a_1 = N/3$. In case N is a multiple of 3, there exist one-parameter families of degenerate stationary points [17]. For simplicity we exclude this situation in all that follows. $\lozenge$

Proposition 3.1 yields the following classification of local minima and saddles of index 1:

1. Local minima $x^\star \in \mathcal{S}_0$ necessarily have triple $(0, a, N - a)$ with $N/3 < a \leqslant N/2$.
2. Saddles of index 1 either have triple $(1, a, N - a - 1)$ with $N/3 < a \leqslant (N - 1)/2$, or they have triple $(N - 2 - a, a, 2)$ with $N/2 - 1 \leqslant a \leqslant 2$ and $a < N/3$. The latter case can only occur if $N = 4$, and corresponds to the triple $(1, 1, 2)$.

Example 3.3 (The case $N = 4$)**.** If $N = 4$, then $\mathcal{S}_0$ contains 6 points, consisting of all possible permutations of $(1, 1, -1, -1)$. In addition, there are 12 saddles of index 1, consisting of all possible permutations of $(1, -1, 0, 0)$. Each of these saddles connects the two local minima obtained by replacing one 0 by 1 and the other one by -1, and vice versa [22, 17, Section 2.4]. The associated transition graph is an octahedron (Figure 3). $\blacklozenge$

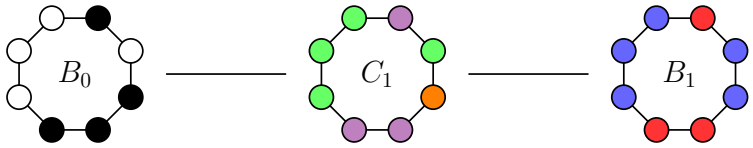

FIGURE 4. Example of transition rules for $N = 8$. The coordinates for family B_0 are ● $= 1$ and ○ $= -1$. Those for C_1 are ● $= -1/\sqrt{7}$, ● $= 3/\sqrt{7}$ and ● $= -2/\sqrt{7}$. Those for B_1 are ● $= 5/\sqrt{19}$ and ● $= -3/\sqrt{19}$.

We will henceforth limit the discussion to the case where $N = 2M$ is even, $N \geqslant 8$ and N is not a multiple of 3. Then the 1-saddles necessarily correspond to triples of the form $(1, a, N - a - 1)$. In order to ease notations, we write $k_{\max} = \lfloor N/6 \rfloor$ and

- B_k for the set of all local minima with triple $(0, M - k, M + k)$, where $k \in [\![0, k_{\max}]\!]$;
- C_k for the set of all 1-saddles with triple $(1, M - k, M + k - 1)$, where $k \in [\![1, k_{\max}]\!]$.

Simple combinatorics shows that the cardinalities of these families are

$$|B_0| = \binom{2M}{M}, \qquad |B_k| = 2\binom{2M}{M+k}, \qquad |C_k| = \frac{2(2M)!}{1!(M-k)!(M+k-1)!} \tag{3.4}$$

where $k \in [\![1, k_{\max}]\!]$. The factors 2 are due to the fact that except for B_0, there are always two choices for the signs of coordinates.

One can obtain explicit expressions for the coordinates of all these stationary points, see (A.3) in Appendix A.1. Here it will suffice to know that local minima in B_0 simply have M coordinates equal to $+1$ and M coordinates equal to -1. These stationary points are expected, and admit a simple interpretation in terms of a particle system: we just associate each coordinate equal to $+1$ with the presence of a particle, and each coordinates equal to -1 with the absence of a particle, that is, a hole.

The other families of local minima $B_1, \ldots, B_{k_{\max}}$ have more complicated coordinates, which do not allow for an interpretation as a particle system. In fact their presence comes a bit as a surprise, so that we will call them *spurious* configurations. We will however show below that they have a higher energy than the configurations in B_0, and therefore they will not play an important rôle when the system is observed on a sufficiently long timescale.

Example 3.4 (The case $N = 8$)**.** If $N = 8$, there are two families of local minima B_0 and B_1, and one family of 1-saddles C_1 (Figure 4).

- The family of local minima B_0 corresponds to the triple $(0, 4, 4)$, and contains all points that have 4 coordinates equal to $+1$ and 4 coordinates equal to -1. They can thus be interpreted as configurations with 4 particles and 4 holes.
- The family of local minima B_1 corresponds to the triple $(0, 3, 5)$. It contains all points with 3 coordinates equal to $5/\sqrt{19}$ and 5 coordinates equal to $-3/\sqrt{19}$, as well as all configurations with opposite signs.
- The family of 1-saddles C_1 corresponds to the triple $(1, 3, 4)$. It contains all points with 1 coordinate equal to $-1/\sqrt{7}$, 3 coordinates equal to $3/\sqrt{7}$ and 4 coordinates equal to $-2/\sqrt{7}$, as well as all configurations with opposite signs. ♦

Now that we have determined all stationary points in $\mathcal{S}_0$ and $\mathcal{S}_1$, we have to find the structure of the transition graph $\mathcal{G} = (\mathcal{S}_0, \mathcal{E})$. In other words, we have to determine which local minima are connected by a given 1-saddle. This question is answered in the following result.

Theorem 3.5 (Transition graph for $\gamma = 0$)**.** *Each* 1*-saddle in* C_k *connects exactly one local minimum in* B_{k-1} *with one local minimum in* B_k*. More precisely, if the coordinates of the saddle have values* $\alpha'_0, \alpha'_1, \alpha'_2$*, and those of the local minima are respectively* α_1, α_2 *and* α''_1, α''_2*, then the connection rules are given by*

$$\begin{aligned} &\alpha_1 \longleftrightarrow \alpha'_0 \longleftrightarrow \alpha''_2 && 1 \text{ coordinate}, \\ &\alpha_1 \longleftrightarrow \alpha'_1 \longleftrightarrow \alpha''_1 && M-k \text{ coordinates}, \\ &\alpha_2 \longleftrightarrow \alpha'_2 \longleftrightarrow \alpha''_2 && M+k-1 \text{ coordinates}. \end{aligned} \tag{3.5}$$

We give the proof in Appendix A.1. It is based on the construction of two continuous paths connecting a given point in C_k to one point in B_{k-1} and one point in B_k, such that the potential decreases along the path when moving away from the saddle. Figure 4 illustrates the connection rule in the case $N = 8$. See also [5, Fig. 5].

Using the relations (3.4), one easily checks that the number of saddles in C_k is indeed equal to the number of allowed connections between elements in B_{k-1} and C_k as well as B_k and C_k.

3.3 The case of weak positive coupling

It follows from basic perturbation arguments that the transition graph $\mathcal{G}$ will persist for small positive coupling intensity γ. Indeed, if we assume that N is not a multiple of 3, then all stationary points for $\gamma = 0$ are nondegenerate, so that the implicit function theorem shows that they still exist for small positive coupling, and move at most by a distance of order γ. In addition, perturbation results for the eigenvalues of matrices such as the Bauer–Fike theorem (see for instance [21]) show that the signature of nondegenerate stationary points does not change for small γ. Finally, the proof of Theorem 3.5 essentially relies on the relation (A.10), whose coefficients depend continuously on γ.

The drawback of this argument is that while it shows that for any $N < \infty$, there exists a critical coupling $\gamma^*(N) > 0$ such that the transition graph does not change for $0 \leqslant \gamma < \gamma^*(N)$, it does not yield a good control on the critical coupling as $N \to \infty$. To obtain a lower bound on $\gamma^*(N)$ which is uniform in N (at least for k fixed), we adapt from [6] an argument based on symbolic dynamics to obtain the following result.

Theorem 3.6 (Persistence of the transition graph for small positive γ)**.** *There exists a constant* $c > 0$*, independent of* N*, such that the stationary points of the families* B_k *and* C_k *persist for*

$$\gamma \leqslant c\left(\frac{1}{6} - \frac{k}{N}\right)^2, \tag{3.6}$$

without changing their index. In the particular case of stationary points of the family B_0*, we have the sharper result that they persist at least as long as* $\gamma < \frac{7}{3} - \sqrt{5} \simeq 0.097$*.*

The proof is given in Appendix A.2. It also provides a criterion allowing to sharpen the bound (3.6) for families other than B_0, cf. (A.38), which however is not essential in what follows.

The important aspect of this result is that all families of stationary points B_k or C_k with $\frac{k}{N}$ bounded away from $\frac{1}{6}$ are ensured to exist up to a positive critical coupling independent of N. Only stationary points with $k = \frac{N}{6} - o(N)$ might disappear at a critical γ which vanishes in the large-N limit.

4 Metastable hierarchy

Now that the structure of the transition graph $\mathcal{G}$ is understood, we have access to information on timescales of the metastable process. A convenient way of doing this relies on the concept of *metastable hierarchy*, which is an ordering of the local minima from deepest to shallowest. We summarise this construction in Section 4.1, before applying it to our case in Section 4.2. A more refined hierarchy can be obtained for small positive coupling γ among the local minima of the family B_0, which have a particle interpretation; we do this in Section 4.3.

4.1 Metastable hierarchy and Eyring–Kramers law

We consider in this section a general reversible diffusion process in $\mathbb{R}^N$ of the form (2.2), with potential V of class $\mathcal{C}^2$.

Definition 4.1 (Communication height)**.** *Let $x^\star$ be a local minimum of V and let $A \subset \mathbb{R}^N$. The* communication height *from $x^\star$ to A is the nonnegative number*

$$H(x^\star, A) = \inf_{\gamma : x^\star \to A} \sup_{t \in [0,1]} V(\gamma(t)) - V(x^\star) \, , \tag{4.1}$$

where the infimum runs over all continuous paths $\gamma : [0,1] \to \mathbb{R}^N$ such that $\gamma(0) = x^\star$ and $\gamma(1) \in A$. Any path γ realising (4.1) *is called a* minimal path *from $x^\star$ to A.*

The communication height measures how high one cannot avoid climbing in the potential landscape to go from $x^\star$ to A. Assuming A does not intersect the basin of attraction of $x^\star$ and all stationary points of V are nondegenerate, it is not difficult to show that the supremum in (4.1) is reached at a 1-saddle $z^\star$ of V (see for instance [8, Section 2]). In that case, one has $H(x^\star, A) = V(z^\star) - V(x^\star)$.

A notion of metastable order of local minima was introduced in [11]. In our case, due to the fact that many minima have the same or almost the same potential value, we introduce the following generalisation of this concept to partitions of the set of local minima. Typically, we will apply this definition to cases where the points in each element of the partition have approximately or exactly the same potential height.

Definition 4.2 (Metastable hierarchy of a partition)**.** *A partition $\mathcal{S}_0 = P_1 \cup P_2 \cup \ldots \cup P_m$ of the set $\mathcal{S}_0$ of local minima of V is said to form a* metastable hierarchy *if there exists a constant $\theta > 0$ such that for all $k \in [\![2, m]\!]$, one has*

$$H\biggl(x^\star, \bigcup_{i=1}^{k-1} P_i\biggr) \leqslant \min_{y^\star \in P_\ell} H\biggl(y^\star, \bigcup_{i=1}^{k} P_i \setminus P_\ell\biggr) - \theta \tag{4.2}$$

for all $x^\star \in P_k$ and all $\ell \in [\![1, k-1]\!]$. In this case, we write

$$P_1 \prec P_2 \prec \cdots \prec P_m \, . \tag{4.3}$$

In words, it is easier, starting in any point in P_k, to reach a lower-lying set P_ℓ in the hierarchy than it is, starting in such an P_ℓ, to reach any other set among $P_1, \ldots P_k$. A graphical way of constructing the hierarchy relies on the so-called *disconnectivity tree* [12]; it is illustrated in Figure 5 in a simple case where all $P_k = \{x_k^\star\}$ are singletons. The leaves of the tree have coordinates $(x_k^\star, V(x_k^\star))$; each leaf is connected to the lowest

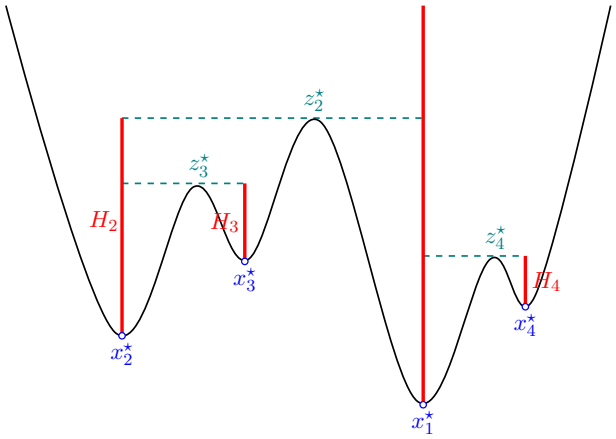

FIGURE 5. Example of a 4-well potential, with its disconnectivity tree. The metastable order is given by $x_1^\star \prec x_2^\star \prec x_3^\star \prec x_4^\star$. The communication heights $H_k = H(x_k^\star, \{x_1^\star, \dots, x_{k-1}^\star\}) = V(z_k^\star) - V(x_k^\star)$ provide the Arrhenius exponents for mean transition times and small eigenvalues of the generator $\mathcal{L}$. Prefactors in the Eyring–Kramers law (4.4) are given in terms of second derivatives of the potential at the local minima $x_k^\star$ and 1-saddles $z_k^\star$.

saddle reachable from it, and the procedure is repeated after discarding the shallower local minimum whenever two branches join.

In the particular case where all P_k are singletons, the following result by Bovier, Gayrard and Klein connects the metastable hierarchy with certain first-hitting times and with small eigenvalues of the infinitesimal generator $\mathcal{L} = \varepsilon\Delta - \nabla V(x) \cdot \nabla$ of the diffusion.

Theorem 4.3 (Eyring–Kramers law for nondegenerate potentials [11])**.** *Assume the local minima of V admit a metastable order $x_1^\star \prec \cdots \prec x_m^\star$. For each $k \in [\![1, m]\!]$, denote by τ_k the first-hitting time of the ε-neighbourhood of $\{x_1^\star, \dots, x_k^\star\}$, and let λ_k by the kth smallest eigenvalue of $-\mathcal{L}$. Assume further that for each k, there is a unique 1-saddle $z_k^\star$ such that any minimal path from $x_k^\star$ to $\{x_1^\star, \dots, x_{k-1}^\star\}$ reaches communication height only at $z_k^\star$. Then for each $k \in [\![2, m]\!]$, one has*

$$\mathbb{E}^{x_k^\star}[\tau_{k-1}] = \frac{2\pi}{|\lambda_-(z_k^\star)|} \sqrt{\frac{|\det \nabla^2 V(z_k^\star)|}{\det \nabla^2 V(x_k^\star)}}\, \mathrm{e}^{[V(z_k^\star) - V(x_k^\star)]/\varepsilon} \big[1 + \mathcal{O}(\varepsilon^{1/2} |\log \varepsilon|^{3/2})\big] \,, \tag{4.4}$$

where $\nabla^2 V(x)$ denotes the Hessian matrix of V at x, and $\lambda_-(z_k^\star)$ is the unique negative eigenvalue of $\nabla^2 V(z_k^\star)$. Furthermore, $\lambda_1 = 0$ and there exists a constant $\theta_1 > 0$ such that

$$\lambda_k = \frac{1}{\mathbb{E}^{x_k^\star}[\tau_{k-1}]} \big[1 + \mathcal{O}(\mathrm{e}^{-\theta_1/\varepsilon})\big] \tag{4.5}$$

holds for all $k \in [\![2, m]\!]$.

This result tells us in particular that if the system starts at a stationary point at the end of the metastable hierarchy, it will spend longer and longer amounts of time going down the hierarchy (possibly visiting other local minima in between), before reaching the ground state $x_1^\star$. In particular, the spectral gap $\lambda_2 - \lambda_1 = \lambda_2$ of the system, which gives the exponential rate of convergence to equilibrium, depends to leading order only on the second local minimum in the hierarchy $x_2^\star$, and on the saddle $z_2^\star$ connecting it to the ground state.

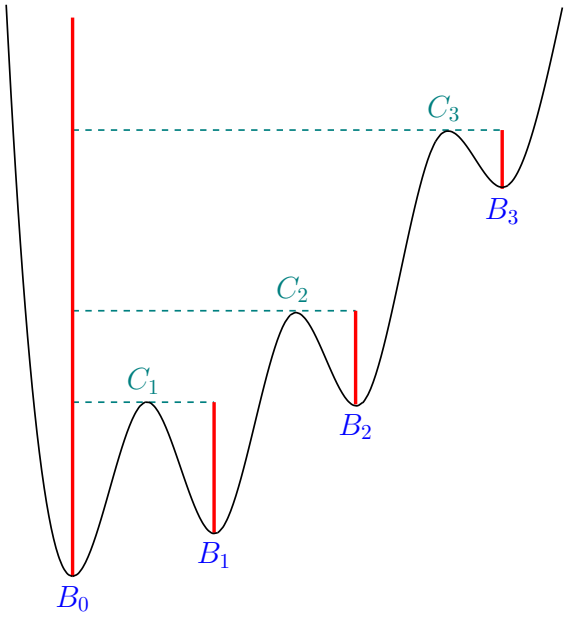

FIGURE 6. Value of the potential V_0 along a path $B_0 \to C_1 \to B_1 \to \dots$ in the case $N = 20$ (not to scale). The associated disconnectivity tree shows that the B_k are indeed in metastable order. Thus the long-time dynamics will concentrate on the set B_0 of particle–hole configurations.

4.2 Hierarchy on the families B_k

Unfortunately, Theorem 4.3 does not apply to our situation, because one cannot find a hierarchy for singletons. This is due to the fact that the potential V_γ has many symmetries, and therefore many stationary points have the same potential height, preventing us from fulfilling (4.2) with a positive θ. In particular, in the uncoupled case $\gamma = 0$, the system is invariant under the group $G = \mathfrak{S}_N \times \mathbb{Z}_2$, where $\mathfrak{S}_N$ is the symmetric group describing permutations of the N coordinates, and the factor $\mathbb{Z}_2 = \mathbb{Z}/2\mathbb{Z}$ accounts for the $x \mapsto -x$ symmetry. The families B_k and C_k each form a group orbit under G, that is, they are equivalence classes of the form $\{gx \colon g \in G\}$.

However, we will be able to draw on results of [5], which generalise Theorem 4.3 to Markovian jump processes invariant under a group of symmetries, and the extension of these results to diffusion processes [17, 16]. In particular, [5, Thm 3.2] shows that if the system starts with an initial distribution which is uniform on some B_k, then a very similar result to Theorem 4.3 holds true. The only difference is that the prefactor in the Eyring–Kramers law (4.4) has to be multiplied by a factor which can be explicitly computed in terms of stabilisers of the group orbits.

The following result provides a metastable order on the B_k, which is exactly what is required to apply the theory from [5, 17, 16] in the uncoupled case.

Theorem 4.4 (Metastable hierarchy on the B_k)**.** *If $\gamma = 0$, then the families B_k satisfy a metastable order given by*

$$B_0 \prec B_1 \prec \cdots \prec B_{k_{\max}} \,. \tag{4.6}$$

Furthermore, any minimal path from B_k to B_{k-1} reaches communication height only on saddles in C_k. The hierarchy (4.6) *still applies for sufficiently small positive γ, the only*

difference being that all points inside a given B_k do not necessarily have the same potential value.

We give the proof in Appendix B.1. The situation is illustrated in Figure 6. As k increases from 0 to $k_{\max}$, the potential height of the B_k increases, while the barrier height between C_k and B_k decreases. See Appendix B.1 for explicit expressions for these potential values. Applying [5, Thm 3.2], we obtain in particular the following result.

Corollary 4.5. *For $k \in [\![1, k_{\max}]\!]$, let τ_{k-1} be the first-hitting time of the ε-neighbourhood of $B_0 \cup \cdots \cup B_{k-1}$. If the initial distribution μ of the system is concentrated on $B_k \cup \cdots \cup B_{k_{\max}}$ and invariant under G, then for $\gamma = 0$ one has*

$$\mathbb{E}^{\mu}[\tau_{k-1}] = \frac{2\pi}{|\lambda_-(z_k^\star)|(M+k)} \sqrt{\frac{|\det \nabla^2 V_0(z_k^\star)|}{\det \nabla^2 V_0(x_k^\star)}}\, \mathrm{e}^{[V_0(z_k^\star) - V_0(x_k^\star)]/\varepsilon} \bigl[1 + \mathcal{O}(\varepsilon^{1/2} |\log \varepsilon|^{3/2})\bigr] \ , \quad (4.7)$$

where $x_k^\star$ is any local minimum in B_k, $z_k^\star$ is any saddle in C_k, and $M = N/2$.

Proof: Theorem 3.2 in [5] shows that in the case of a symmetric initial distribution, the usual Eyring–Kramers formula (4.4) has to be multiplied by the factor $|G_{x_k^\star} \cap G_{x_{k-1}^\star}|/|G_{x_k^\star}|$, where $G_x = \{g \in G \colon g(x) = x\}$ is the stabiliser of x. If $k \geqslant 1$, then $|G_{x_k^\star}|$ is the number of permutations that leave invariant any element in B_k, and is equal to $(M-k)!(M+k)!$. Similarly, $|G_{x_k^\star} \cap G_{x_{k-1}^\star}|$ is the number of permutations leaving invariant any two elements in B_k and B_{k-1} connected in the transition graph $\mathcal{G}$, which is equal to $(M-k)!(M+k-1)!$. □

Note the extra factor $(M+k)^{-1}$ in (4.7). In fact, $M+k$ is also the number of saddles in C_k that are connected with any given element of B_k (cf. [5, Eq. (2.25)]). The interpretation of this factor is that since the system has $M+k$ different ways to make a transition from a given $x_k^\star \in B_k$ to B_{k-1}, the transition time is divided by this factor.

The above result will still apply for small positive coupling, but with a more complicated expression for the prefactor. This is because the system is no longer invariant under $\mathfrak{S}_N \times \mathbb{Z}_2$, but under the smaller group $\mathfrak{D}_N \times \mathbb{Z}_2$, where $\mathfrak{D}_N$ is the dihedral group of symmetries of a regular N-gon. The important aspect for us is that we still have a control of the time needed to reach the family of stationary points B_0, which lie at the bottom of the hierarchy and have an interpretation in terms of particle–hole configurations. The dynamics among configurations in B_0 is much slower than the relaxation towards B_0, because it involves crossing the potential barrier from B_0 to B_1 via C_1. We will analyse it in more detail in the next section.

4.3 Hierarchy on B_0 and particle interpretation

We assume in this section that $0 < \gamma \ll \gamma_{\mathrm{c}}$, where γ_{c} is the critical coupling below which all stationary points in B_0, B_1 and C_1 exist without bifurcating. The central observation in order to classify points in B_0 is that if $x^\star(\gamma)$ is any critical point of V_γ, then

$$V_\gamma\bigl(x^\star(\gamma)\bigr) = V_0\bigl(x^\star(0)\bigr) + \frac{\gamma}{4} \sum_{i=1}^{N} \bigl(x_{i+1}^\star(0) - x_i^\star(0)\bigr)^2 + \mathcal{O}(\gamma^2) \ . \quad (4.8)$$

This is because $V_0(x^\star(\gamma)) = V_0(x^\star(0)) + \mathcal{O}(\gamma^2)$, as the first-order term in γ vanishes since $\nabla V_0(x^\star(0)) = \lambda \mathbf{1}$ is orthogonal to $x^\star(\gamma) - x^\star(0)$, which belongs to the hyperplane S. The first term on the right-hand side of (4.8) is constant on each B_k and each C_k. The second term

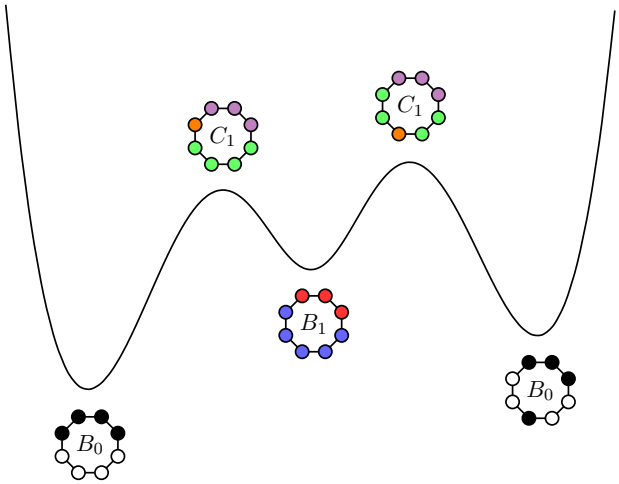

FIGURE 7. Example of an allowed transition, from a configuration in B_0 with two interfaces to a configuration in B_0 with 4 interfaces. The net effect is that a particle has hopped by two sites.

is determined by the number of nearest-neighbour coordinates of $x^\star(0)$ that are different, which we are going to call *interfaces* of the configuration.

In particular, if $x^\star(0) \in B_0$, we know that all its components have values ± 1. We define its number of interfaces as

$$I_{1/-1}(x^\star) = \sum_{i=1}^{N} 1_{\{x_i^\star(0) \neq x_{i+1}^\star(0)\}} \tag{4.9}$$

so that we have

$$V_\gamma\big(x^\star(\gamma)\big) = V_0\big(x^\star(0)\big) + \gamma I_{1/-1}(x^\star) + \mathcal{O}(\gamma^2) \tag{4.10}$$

where $V_0(x^\star(0)) = -\frac{1}{4}N$. Furthermore, we define the number of interfaces at site i as

$$I_{1/-1}(x^\star, i) = 1_{\{x_{i-1}^\star(0) \neq x_i^\star(0)\}} + 1_{\{x_i^\star(0) \neq x_{i+1}^\star(0)\}} \in \{0, 1, 2\} \, . \tag{4.11}$$

Interpreting each 1 as a particle and each -1 as a hole, it is natural to introduce the following terminology:

- a site i with 2 interfaces will be called an *isolated* particle or hole;
- a sequence of at least 2 contiguous particles or holes will be called a *cluster*;
- a site with 1 interface lies at the *boundary of a cluster*;
- a site without interface belongs to the *bulk of a cluster*.

Lemma 4.6. *Let $x^\star$ be a critical point in B_0 and write $M = \frac{N}{2} \geqslant 4$. Then the following properties hold.*

1. *The total number of interfaces $I_{1/-1}(x^\star)$ is even.*
2. *If $I_{1/-1}(x^\star) = 2$, then $x^\star$ consists in a cluster of M particles and a cluster of M holes.*
3. *If $I_{1/-1}(x^\star) > M$, then $x^\star$ has at least one isolated site.*
4. *Among the $x^\star \in B_0$ with $I_{1/-1}(x^\star) \in [\![4, M]\!]$, there exist both configurations with isolated sites and configurations without isolated sites.*

PROOF: Denote by N_c the number of clusters, by N_i the number of isolated sites, and by $p = I_{1/-1}(x^\star)$ the number of interfaces. Then we have $p = N_\mathrm{c} + N_\mathrm{i}$, which is necessarily

even. Since clusters have at least two sites, $N \geqslant 2N_{\mathrm{c}} + N_{\mathrm{i}}$, implying $N_{\mathrm{c}} \leqslant N - p$ and thus $N_{\mathrm{i}} \geqslant 2p - N$. Thus if $p > M$, then $N_{\mathrm{i}} > 0$. If $4 \leqslant p \leqslant M$, then a possible configuration consists in $p-2$ clusters of size 2, leaving at least 4 sites that can be split into 2 more clusters. Another possibility is to have $p-2$ isolated sites, leaving at least $N-2$ sites that can again be split into 2 clusters. If $p = 2$, we necessarily have 2 clusters of equal size. □

This result motivates the following notation for configurations in B_0:

- A_2 denotes the set of all configurations with interface number $I_{1/-1}(x^\star) = 2$;
- for even $p \in [\![4, M]\!]$, A_p denotes the set of all configurations $x^\star \in B_0$ with p interfaces having at least one isolated site, and A'_p denotes the set of configurations with p interfaces having no isolated site;
- for even $p \in [\![M+1, N]\!]$, A_p denotes the set of configurations with p interfaces (which all have at least one isolated site).

We now need to determine the communication heights between configurations in these different sets for small positive γ. For this, we have to take into account the fact that any transition between two configurations in B_0 involves crossing two 1-saddles in C_1, separated by an element of B_1 (Figure 7). The communication height will thus be determined by the highest of the two saddles. Examining the different possible cases yields the following result, which is proved in Appendix B.2.

Proposition 4.7 (Transitions between configurations in B_0)**.** *Let $x_1^\star(\gamma), x_2^\star(\gamma) \in B_0$ be two particle/hole configurations, and denote by $p = I_{1/-1}(x_1^\star(0))$ the number of interfaces of $x_1^\star(0)$. Then a transition between these configurations is possible if and only if $x_2^\star(0)$ is obtained by interchanging a particle and a hole in $x_1^\star(0)$. The interface number of $x_2^\star(0)$ satisfies*

$$I_{1/-1}\big(x_2^\star(0)\big) \in \{p-4, p-2, p, p+2, p+4\} \,. \tag{4.12}$$

The communication height from $x_1^\star(\gamma)$ to $x_2^\star(\gamma)$ admits the expansion

$$H\big(x_1^\star(\gamma), x_2^\star(\gamma)\big) = H^{(0)} + \gamma H^{(1)}\big(x_1^\star(0), x_2^\star(0)\big) + \mathcal{O}(\gamma^2) \,, \tag{4.13}$$

where

$$H^{(0)} = V_0(C_1) - V_0(B_0) = \frac{M(M-1)}{4(M^2 - 3M + 3)} \tag{4.14}$$

depends only on $M = \frac{N}{2}$, while $H^{(1)}(x_1^\star(0), x_2^\star(0))$ also depends on p and on the number of interfaces of the two exchanged sites as detailed in Table 1.

Table 1 shows that all allowed transitions between particle/hole configurations have simple physical interpretations. In particular, only the last four types of transitions decrease the number of interfaces. Types V.b and V.c can be viewed as an isolated particle merging with another particle (isolated or at the boundary of a cluster), type V.a as a particle splitting from another one to fill a hole between two particles, and type VI as an isolated particle jumping into a hole between two particles. Types I and II are just the reversed versions of types VI and V, while all transitions of type III and IV are their own reverse.

Figure 8 shows the allowed transitions in the case $N = 8$; only transitions that minimise the communication height are shown. Figure 9 shows the case $N = 16$. Note that in accordance with Lemma 4.6, only configurations with $p \leqslant M$ interfaces appear in the two types A_p (with isolated particles and/or holes) and A'_p (without isolated particles and/or holes).

	Transition	Δp	$H^{(1)}\big(x_1^\star(0), x_2^\star(0)\big)$	Saddle
I	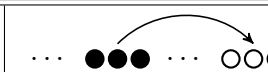	$+4$	$\dfrac{10M^2 - 36M + 36 - 3p}{4(M^2 - 3M + 3)}$	$[0, 2, p+2]$
II.a		$+2$	$\dfrac{2(M-3)^2 - 3p}{4(M^2 - 3M + 3)}$	$[0, 2, p]$
II.b				
II.c	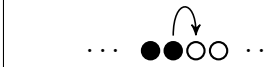			
III		0	$\dfrac{-2M^2 + 6M - 3p}{4(M^2 - 3M + 3)}$	$[1, 1, p-1]$
IV.a		0	$\dfrac{-6M^2 + 12M - 3p}{4(M^2 - 3M + 3)}$	$[0, 2, p-2]$
IV.b				
IV.c	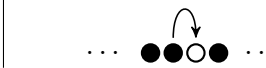			
IV.d	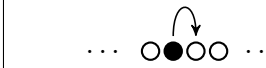			
V.a		-2		
V.b				
V.c	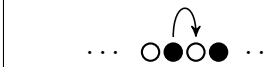			
VI	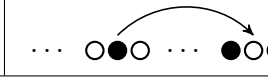	-4		

TABLE 1. List of allowed transitions between elements of B_0, viewed as a particle moving into a hole. The different columns show, respectively, the type of transition, the change Δp of the number of interfaces, the first-order correction to the communication height, and the numbers of interfaces of types α_0'/α_1', α_0'/α_2' and α_1'/α_2' of the highest saddle encountered during the transition (cf. Appendix B.2).

The first-order correction $H^{(1)}$ to communication heights depends not only on the number M of particles, but also on the number p of interfaces. This is a nonlocal effect of the mass-conservation constraint. However, in the limit $M \to \infty$, the four possible corrections converge respectively to $\frac{5}{2}$, $\frac{1}{2}$, $-\frac{1}{2}$ and $-\frac{3}{2}$, i.e. they no longer depend on p.

With this information at hand, it is now possible to determine the metastable hierarchy among the families A_p and A_p'. The result, which is proved in Appendix B.2, reads as follows.

Theorem 4.8 (Metastable hierarchy of particle/hole configurations)**.** *Let M' be the largest even number less or equal $M = \frac{N}{2}$. Then*

$$A_2 \prec A_4' \prec A_6' \prec \cdots \prec A_{M'-2}' \prec A_{M'}' \prec A_4 \prec A_6 \prec \cdots \prec A_{N-2} \prec A_N \,. \tag{4.15}$$

defines a metastable order of the families A_p and A_p'.

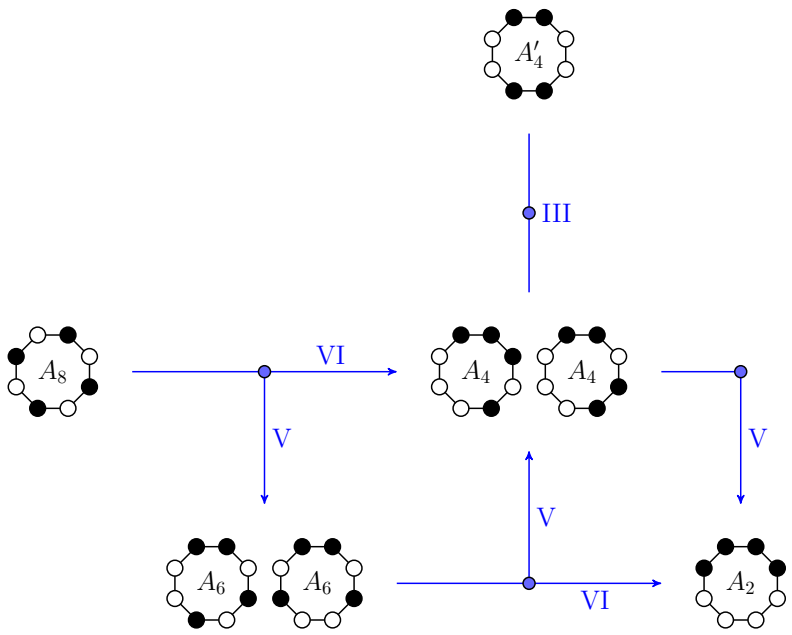

FIGURE 8. Minimal transitions between particle/hole configurations in B_0 for $N = 8$. Arrows indicate transitions that decrease the energy, and are labelled according to Table 1. Each node displays only one representative of an orbit for the group action of $\mathfrak{D}_N \times \mathbb{Z}_2$. The other elements of an orbit are obtained by applying rotations, reflections and interchanging particles and holes. Blue nodes represent stationary points in B_1. Not shown are transitions within the families A_p and A_p', which are of type III or IV.

5 Analysis of the dynamics

5.1 Interface dynamics

The transition rules and communication heights given in Proposition 4.7 and the metastable hierarchy obtained in Theorem 4.8 yield complementary information on the dynamics between particle/hole configurations in B_0. Recall that the process behaves essentially as a Markovian jump process with transition rates of order $\mathrm{e}^{-H(x_i^\star, x_j^\star)/\varepsilon}$, while the hierarchy (4.15) classifies the states according to the time the process spends in them in metastable equilibrium.

At the bottom of the metastable hierarchy, we find the set A_2 of configurations having one cluster of M particles: this constitutes the ground state of the system, which can be interpreted as a solid or condensed phase. At the top of the hierarchy on B_0, we find the set A_N of states with N interfaces. These consist in M isolated particles, and can be interpreted as a gaseous phase.

The transition graph implied by Proposition 4.7 (and illustrated in Figures 8 and 9) shows that when starting in the configuration A_N, the most likely transitions gradually decrease the number p of interfaces, in steps of 2 or 4. Thus the system tends to gradually build clusters of increasing size. As the communication heights given in Table 1 increase as p decreases, this condensation process becomes slower as the size of clusters increases. This is different from the usual Kawasaki dynamics, in which the transition rates depend only on the change Δp of the number of interfaces. Note in particular that for given p, transitions of type IV, V and VI all occur at the same rate.

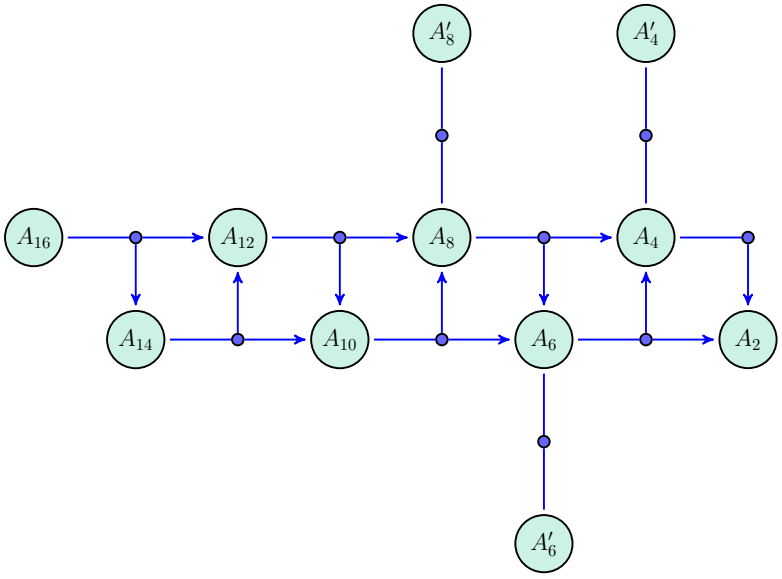

FIGURE 9. Minimal transitions between particle/hole configurations in B_0 in the case $N = 16$. Arrows indicate transitions that decrease the energy.

When the number p of interfaces reaches M (meaning that there are on average 2 particles per cluster), new configurations A'_p become possible. These consist of p clusters separated by at least 2 sites, and appear as dead ends on the transition graph. The metastable order (4.15) shows that these configurations are actually more stable than those of type A_p, $p \geqslant 4$, which have isolated particles or holes, and act as gateways to configurations with fewer interfaces. In particular, configurations in A'_4 are those with the longest metastable lifetime. The system can spend considerable time trapped in configurations with $p \geqslant 2$ clusters of particles, separated by p clusters of holes (as seen in Figure 1).

5.2 Spectral gap

Another interesting information on the process that can be obtained from its metastable hierarchy is its spectral gap. We already know that the generator $\mathcal{L}$ admits the eigenvalue 0, which is associated with the invariant distribution (2.9). This eigenvalue is simple because the process is irreducible and positive recurrent. The spectral gap is thus given by the smallest nonzero eigenvalue λ_2 of $-\mathcal{L}$, which governs the rate of relaxation to equilibrium.

At first glance, one might think that the spectral gap has order $\mathrm{e}^{-(V_\gamma(z^\star)-V_\gamma(y^\star))/\varepsilon}$, where $z^\star$ is a 1-saddle in C_1 and $y^\star$ is a local minimum in B_1. Indeed, this is the inverse of the longest transition time obtained in Corollary 4.5. However, the corollary only applies to symmetric initial distributions, and transitions from B_1 to B_0 via C_1 are not the slowest processes of the system. In fact, this role is played by transitions between configurations in A_2, which occur via saddles in C_1, leading to a spectral gap of order $\mathrm{e}^{-(V_\gamma(z^\star)-V_\gamma(x^\star))/\varepsilon}$, where $x^\star$ is a local minimum in A_2 rather than B_1. Applying the theory for symmetric processes in [5], we obtain the following result. Its proof is given in Appendix C.

Theorem 5.1 (Spectral gap)**.** *If ε is small enough, then the smallest nonzero eigenvalue*

of $-\mathcal{L}$ is given by

$$\lambda_2 = 4\sin^2\left(\frac{\pi}{N}\right)\frac{|\lambda_-(z^\star)|}{2\pi}\sqrt{\frac{\det\nabla^2 V_\gamma(x^\star)}{|\det\nabla^2 V_\gamma(z^\star)|}}\,\mathrm{e}^{-[V_\gamma(z^\star)-V_\gamma(x^\star)]/\varepsilon}\big[1+\mathcal{O}(\varepsilon^{1/2}|\log\varepsilon|^{3/2})\big]\;, \quad (5.1)$$

where $x^\star$ is any configuration in A_2, and $z^\star$ is any saddle in C_1 whose limit as $\gamma\to 0$ has exactly 3 interfaces. In particular, we have

$$\begin{aligned} V_\gamma(z^\star) - V_\gamma(x^\star) &= \frac{M(M-1)}{4(M^2-3M+3)} + \gamma\,\frac{M^2-6M+6}{2(M^2-3M+3)} + \mathcal{O}(\gamma^2) \\ &= \frac{1}{4} + \frac{1}{2}\gamma + \mathcal{O}(N^{-1}) + \mathcal{O}(\gamma^2)\;. \end{aligned} \quad (5.2)$$

Furthermore,

$$\begin{aligned} |\lambda_-(z^\star)|\sqrt{\frac{\det\nabla^2 V_\gamma(x^\star)}{|\det\nabla^2 V_\gamma(z^\star)|}} &= \sqrt{2}\left[\frac{M^2-3M+3}{(M-\frac{3}{2})\sqrt{M(M-3)}}\right]^{M-2} + \mathcal{O}(\gamma) \\ &= \sqrt{2} + \mathcal{O}(N^{-1}) + \mathcal{O}(\gamma)\;. \end{aligned} \quad (5.3)$$

The fact that the spectral gap (5.1) decays like N^{-2} for large N is highly nontrivial. It is related to the fact that the symmetry group $\mathfrak{D}_N \times \mathbb{Z}_2$ admits irreducible representations of dimension 2, and its computation requires the full power of the theory developed in [5].

Physically, this result means that some transitions between states in A_2 require a time of order $N^2\,\mathrm{e}^{1/4\varepsilon}$, i.e., increasing as the square of the system size when the noise intensity ε is constant. In other words, the motion of interfaces slows down like N^{-2} when the system becomes large.

6 Conclusion

Let us briefly summarise the main results obtained in this work.

- Using the concept of metastable hierarchy, the long-term dynamics of the system can be reduced to an effective process jumping between particle/hole configurations. These configurations exist as long a the coupling intensity γ is smaller than a critical value, bounded below by a constant independent of the system size.
- The effective dynamics tends to reduce the number of interfaces, and slows down as this number decreases. As soon as the average size of clusters reaches 2, the system can get trapped in configurations without isolated sites, which are more stable than any configuration with isolated sites.
- The spectral gap is of order $N^{-2}\,\mathrm{e}^{-1/4\varepsilon}$, which decreases as the square of the inverse of the system size. This means that transitions between the N configurations forming the ground state A_2 slow down as N increases.

We emphasise that all results obtained here apply for arbitrarily large but finite system size N. In fact, some quantities like the number θ defining the metastable hierarchy go to zero in the limit $N\to\infty$, so that the orders (4.6) and (4.15) only make sense for finite N. We do not claim either that the error terms of order $\varepsilon^{1/2}|\log\varepsilon|^{3/2}$ in (5.1) and (4.7) are uniform in N, though results obtained in a similar situation in [3] indicate that they probably are.

A different situation of interest, not considered here, arises when the coupling intensity γ grows like N^2. Then one expects that the system converges to a mass-conserving Allen–Cahn SPDE on a bounded interval, which has considerably fewer metastable states. Indeed,

an analogous scenario was obtained in [7], where the unconstrained system with $\gamma \sim N^2$ was shown to have only 2 local minima, and at most $2N$ saddles of index 1. If, by contrast, one has $1 \ll \gamma \ll N^2$, a scaling argument shows that the system should converge to an Allen–Cahn SPDE on a growing domain, which admits more metastable states; see in particular [31, 28] for results in the unconstrained case, and [26] for a recent convergence result in dimension 2.

The behaviour of the constrained system for lattices of dimension larger than 1 remains so far an open problem. The phenomenology is expected to be different, because the energy of clusters then depends not only on the size of their interfaces, but also on the size of their bulk. This can result in scenarios where the interface dynamics accelerates once a critical droplet size has been reached, as is well known for lattice systems with standard Kawasaki dynamics [14].

A Proofs: Potential landscape

A.1 The uncoupled case

Proof of Proposition 3.1. Consider a critical point $x^\star$ of the constrained system with triple (a_0, a_1, a_2). Recall that this means that $x^\star$ has a_j coordinates equal to α_j, $j = 0, 1, 2$, where the α_j are distinct roots of $\xi^3 - \xi - \lambda$ for some $\lambda \in (-\lambda_c, \lambda_c)$. By Vieta's formula, these roots satisfy

$$\alpha_0 + \alpha_1 + \alpha_2 = 0 \,. \tag{A.1}$$

We always have $a_0 + a_1 + a_2 = N$, and by convention $a_0 \leqslant a_1 \leqslant a_2$. Note that we may assume $a_0 \neq a_2$, since otherwise all a_j would be equal, and thus N would be a multiple of 3, which is excluded by assumption.

Combining (A.1) with the constraint $\sum x_i^\star = a_0\alpha_0 + a_1\alpha_1 + a_2\alpha_2 = 0$ yields the relation

$$(a_1 - a_0)\alpha_1 + (a_2 - a_0)\alpha_2 = 0 \,. \tag{A.2}$$

Solving for α_2 and using the fact that all $\alpha_j^3 - \alpha_j$ are equal, a short computation shows that

$$\begin{aligned} \alpha_0 &= \pm(a_1 - a_2)R^{1/2} \,, \\ \alpha_1 &= \pm(a_2 - a_0)R^{1/2} \,, \\ \alpha_2 &= \pm(a_0 - a_1)R^{1/2} \,, \end{aligned} \tag{A.3}$$

where

$$R = \frac{a_2 + a_1 - 2a_0}{(a_1 - a_0)^3 + (a_2 - a_0)^3} = \frac{1}{a_0^2 + a_1^2 + a_2^2 - a_0a_1 - a_0a_2 - a_1a_2} \,. \tag{A.4}$$

We now turn to determining the signature of the Hessian at these critical points of the potential V_γ restricted to the hyperplane S. This signature does not depend on the parametrisation of S, so that it is equal to the signature of the Hessian of

$$\widetilde{V}_\gamma(x_1, \dots, x_{N-1}) = V_\gamma(x_1, \dots, x_{N-1}, -x_1 - \cdots - x_{N-1}) \,. \tag{A.5}$$

Computing the Hessian of $\widetilde{V}_\gamma$ at $x^\star$ shows that it has the form

$$H = \begin{pmatrix} (3\alpha_0^2 - 1)\mathbb{1}_{a_0} & 0 & 0 \\ 0 & (3\alpha_1^2 - 1)\mathbb{1}_{a_1} & 0 \\ 0 & 0 & (3\alpha_2^2 - 1)\mathbb{1}_{a_2 - 1} \end{pmatrix} + (3\alpha_2^2 - 1) \begin{pmatrix} 1 & \cdots & 1 \\ \vdots & \ddots & \vdots \\ 1 & \cdots & 1 \end{pmatrix} \,, \tag{A.6}$$

where $\mathbb{1}_a$ denotes the identity matrix of size a. We now distinguish between the following cases.

1. $(a_0, a_1, a_2) = (0, 0, N)$. Then $x^\star = 0$, and one easily sees that $-H$ is positive definite, so that $x^\star$ is a saddle of index $N-1$.
2. $a_0 = 0$ and $a_1 \geqslant 1$. Using the expressions (A.3), we obtain that $3\alpha_1^2 - 1 > 0$ and $3\alpha_2^2 - 1$ has the same sign as $2a_1 - a_2$. Let $e_1, \dots, e_{N-1}$ denote the canonical basis vectors. Then $\{e_1 - e_i\}_{i \in [\![2, a_1]\!]}$ are eigenvectors of H with eigenvalue $3\alpha_1^2 - 1$, and $\{e_{a_1+1} - e_i\}_{i \in [\![a_1+2, N-1]\!]}$ are eigenvectors of H with eigenvalue $3\alpha_2^2 - 1$.
   To find the remaining two eigenvalues, let $u = \sum_{i=1}^{a_1} e_i$ and $v = \sum_{i=a_1+1}^{N-1} e_i$. These two vectors span an invariant subspace of H, in which the action of H takes the form
   $$\mathcal{M} = \begin{pmatrix} 3\alpha_1^2 - 1 + a_1(3\alpha_2^2 - 1) & (a_2 - 1)(3\alpha_2^2 - 1) \\ a_1(3\alpha_2^2 - 1) & a_2(3\alpha_2^2 - 1) \end{pmatrix}. \tag{A.7}$$
   Computing the determinant and the trace of $\mathcal{M}$, one sees that if $2a_1 > a_2$, then the two eigenvalues of $\mathcal{M}$ are strictly positive, so that $x^\star$ is a stationary point of index 0. If $2a_1 < a_2$, then $\mathcal{M}$ has one strictly positive and one strictly negative eigenvalue, and $x^\star$ has index $a_2 - 1$.
3. $a_0 \geqslant 1$. In that case one finds that $3\alpha_1^2 - 1 > 0$, while $3\alpha_0^2 - 1$ has the same sign as $(2a_2 - a_1 - a_0)(a_0 - 2a_1 + a_2)$ and $3\alpha_2^2 - 1$ has the same sign as $(2a_0 - a_1 - a_2)(a_0 - 2a_1 + a_2)$. Here it is better to invert the rôles of α_1 and α_2 in the expression for H. Similarly to the previous case, one finds $a_0 - 1$ eigenvectors with eigenvalue $3\alpha_0^2 - 1$, $a_2 - 1$ eigenvectors with eigenvalue $3\alpha_2^2 - 1$ and $a_1 - 2$ eigenvectors with eigenvalue $3\alpha_1^2 - 1$ (these eigenvectors are of the form $e_1 - e_i$, $e_{a_0+1} - e_i$ and $e_{a_0+a_2+1} - e_i$ for appropriate ranges of i).
   To find the other eigenvalues, let $u = \sum_{i=1}^{a_0} e_i$, $v = \sum_{i=a_0+1}^{a_0+a_2} e_i$ and $w = \sum_{i=a_0+a_2+1}^{N-1} e_i$. These span an H-invariant subspace, in which the action of H takes the form
   $$\mathcal{M} = \begin{pmatrix} 3\alpha_0^2 - 1 + a_0(3\alpha_1^2 - 1) & a_2(3\alpha_1^2 - 1) & (a_1 - 1)(3\alpha_1^2 - 1) \\ a_0(3\alpha_1^2 - 1) & 3\alpha_2^2 - 1 + a_2(3\alpha_1^2 - 1) & (a_1 - 1)(3\alpha_1^2 - 1) \\ a_0(3\alpha_1^2 - 1) & a_2(3\alpha_1^2 - 1) & a_1(3\alpha_1^2 - 1) \end{pmatrix}. \tag{A.8}$$
   In this case, one finds $\operatorname{Tr} \mathcal{M} > 0$, and $\det \mathcal{M}$ has the same sign as $a_0 - 2a_1 + a_2$. If $\det \mathcal{M} < 0$, then $\mathcal{M}$ has two strictly positive and one strictly negative eigenvalue, and $x^\star$ has index a_0. If $\det \mathcal{M} > 0$, computing the term of degree 1 of the characteristic polynomial of $\mathcal{M}$ one concludes that all eigenvalues of $\mathcal{M}$ are strictly positive, and that $x^\star$ has index $a_2 - 1$. □

Proof of Theorem 3.5. Let $z^\star \in C_k$ be a 1-saddle. Its triple can be written $(1, a-1, N-a)$ where $a = \frac{N}{2} - k + 1 \in [\![\frac{N}{2} + 1 - k_{\max}, \frac{N}{2}]\!]$. We shall construct a path Γ, connecting $z^\star$ to a point $x^\star \in B_{k-1}$ of triple $(0, a, N-a)$, and such that the potential V_0 is decreasing along Γ. An analogous construction holds for the connection from $z^\star$ to a local minimum in B_k.

In fact it will turn out to be sufficient to use a linear path. Reordering the components if necessary, we may assume that $x^\star = (\alpha_1, \dots, \alpha_1, \alpha_2, \dots, \alpha_2)$ with α_1 repeated a times and α_2 repeated $N-a$ times, and $z^\star = (\alpha_0', \alpha_1', \dots, \alpha_1', \alpha_2', \dots, \alpha_2')$, with α_1' repeated $a-1$ times and α_2' repeated $N-a$ times. Note that these points indeed satisfy the connection rules (3.5). Let $\Gamma(t) = tz^\star + (1-t)x^\star$ and set $h(t) = V_0(\Gamma(t))$. Then a direct computation

shows that

$$\begin{aligned} h'(t) = (\alpha_0' - \alpha_1)\big[((1-t)\alpha_1 + t\alpha_0')^3 - ((1-t)\alpha_1 + t\alpha_0')\big] \\ + (a-1)(\alpha_1' - \alpha_1)\big[((1-t)\alpha_1 + t\alpha_1')^3 - ((1-t)\alpha_1 + t\alpha_1')\big] \\ + (N-a)(\alpha_2' - \alpha_2)\big[((1-t)\alpha_2 + t\alpha_2')^3 - ((1-t)\alpha_2 + t\alpha_2')\big] \,. \end{aligned} \tag{A.9}$$

The properties of the α_j and α_j' yield $h'(0) = h'(1) = 0$. Since $h'(t)$ is a polynomial of degree 3, it can be written as

$$h'(t) = Kt(t-1)(t-\psi) \tag{A.10}$$

for some $K, \psi \in \mathbb{R}$. Computing the coefficient of t^3 in (A.9) yields $K > 0$. Thus if we manage to show that $\psi > 1$, we can indeed conclude that $h'(t) < 0$ on $(0,1)$, showing that $h(t)$ is decreasing as required. The condition $\psi > 1$ is equivalent to having $h''(1) < 0$. Using the expressions (A.3) of the α_j, one obtains after some algebra that

$$\begin{aligned} h''(1) = 2(\omega')^2\big[(a-1)(9a-8N) + aN^2 - a^2N\big] - 4\omega\omega' N(N-a)(a-2) - \omega^2 aN(N-a) \\ + 3(\omega\omega')^2(N-a)\big[aN^3 - 3a^2N^2 + 3Na^2 - (a-1)(9a^2 - 9aN + 4N^2)\big] \,, \end{aligned} \tag{A.11}$$

where $\omega = (N^2 - 3aN + 3a^2)^{-1/2}$ and $\omega' = (N^2 - 3aN + 3(a^2 - a + 1))^{-1/2}$ stem from the terms $R^{1/2}$ in (A.3). Using the fact that $\omega\omega' N(N-a)(a-2) > 0$, rearranging and replacing ω and ω' by their values, the condition $h''(1) < 0$ can be seen to be true if the condition $g(a) < 0$ holds, where

$$\begin{aligned} g(a) = 9(8N-27)a^4 + -3(56N^2 - 156N - 81)a^3 + 3N(48N^2 - 101N - 156)a^2 \\ - N^2(56N^2 - 74N - 303)a + 2N^3(4N^2 - 37) \,. \end{aligned} \tag{A.12}$$

To check the condition, first observe that if $N \geqslant 4$ then $g^{(4)}(a) > 0$ for all a. Next check that $g^{(3)}(\frac{N}{2}) < 0$ for $N \geqslant 4$ to conclude that $g^{(3)}(a) < 0$ for all $a \leqslant \frac{N}{2}$. Proceeding in a similar way with the second and first derivatives of g, one reaches the conclusion that $g(a)$ is decreasing for $a \leqslant \frac{N}{2}$ if $N \geqslant 4$. It thus remains to show that g is negative at the left boundary of its domain of definition. This follows by checking the slightly stronger condition $g(\frac{N}{3} + \frac{4}{3}) < 0$. □

A.2 The case of small positive coupling

To prove Theorem 3.6, we proceed in two steps. First we ignore the constraint that stationary points $x^\star$ should belong to the hyperplane S, and prove that the equation

$$\nabla V_\gamma(x) = \lambda \mathbf{1} \tag{A.13}$$

admits exactly 3^N solutions for all (γ, λ) in a given domain. Then we obtain conditions on (γ, λ) guaranteeing that these stationary points belong to S.

Let $\lambda_{\mathrm{c}} = \frac{2}{3\sqrt{3}}$ and define

$$D = \big\{(\gamma, \lambda) \in [0, \tfrac{1}{4}] \times [-\lambda_{\mathrm{c}}, \lambda_{\mathrm{c}}] \colon |\lambda| + \gamma\hat{\alpha}(\lambda) \leqslant \lambda_{\mathrm{c}}(1-\gamma)^{3/2}\big\} \,, \tag{A.14}$$

where $\hat{\alpha}(\lambda)$ is the largest root of $x^3 - x - |\lambda|$. The set D is shown in Figure 10. A simpler sufficient condition for being in D is obtained by observing that

$$D \supset D' = \big\{(\gamma, \lambda) \in [0, \tfrac{2}{9}] \times [-\lambda_{\mathrm{c}}, \lambda_{\mathrm{c}}] \colon |\lambda| \leqslant \lambda_{\mathrm{c}}(1 - \tfrac{9}{2}\gamma)\big\} \,, \tag{A.15}$$

owing to the fact that $\hat{\alpha}(\lambda) \in [1, \frac{2}{\sqrt{3}}]$ for $|\lambda| \leqslant \lambda_{\mathrm{c}}$.

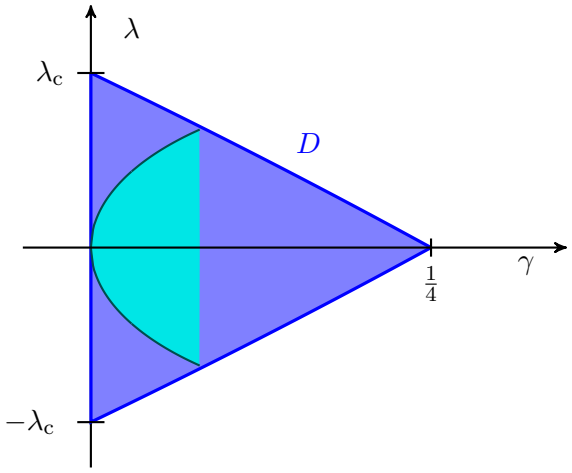

FIGURE 10. The domain D in the (γ, λ)-plane defined in (A.14) (the boundaries of D are not straight line segments, although they look straight). For all $(\gamma, \lambda) \in D$, the equation $\nabla V_\gamma(x) = \lambda \mathbf{1}$ admits 3^N stationary points. The smaller domain corresponds to the parameter values where stationary points of the family B_0 can exist in the hyperplane S.

Proposition A.1. *If $(\gamma, \lambda) \in D$, then* (A.13) *admits exactly 3^N solutions, depending continuously on γ and λ.*

PROOF: The proof, in the spirit of [24], is based on the construction of a horseshoe-type map admitting an invariant Cantor set on which the dynamics is conjugated to the full shift on 3 symbols. First note that we may assume $0 < \gamma \leqslant \frac{1}{4}$, the case $\gamma = 0$ having already been dealt with. Let $f_\lambda(x) = x - x^3 + \lambda$ and consider the map $T : \mathbb{R}^2 \to \mathbb{R}^2$ given by

$$T(x, y) = \Big(2x - y - \frac{2}{\gamma} f_\lambda(x), x\Big) \,. \tag{A.16}$$

This is an invertible map, with inverse $T^{-1} = \Pi \circ T \circ \Pi$ where Π is the involution given by $\Pi(x, y) = (y, x)$. Furthermore, the relation $T(x_n, x_{n-1}) = (x_{n+1}, x_n)$ is equivalent to

$$x_n^3 - x_n - \frac{\gamma}{2}\big(x_{n+1} - 2x_n + x_{n-1}\big) = \lambda \,. \tag{A.17}$$

This shows that fixed points of T^N are in one-to-one correspondence with solutions of (A.13). Our aim is thus to show that when $(\gamma, \lambda) \in D$, the map T has exactly 3^N periodic orbits of (not necessarily minimal) period N. To this end, we construct some subsets of $\mathbb{R}^2$ which behave nicely under the map T.

We can write $T(x, y) = (g(x) - y, x)$ where g is the function

$$g(x) = 2x - \frac{2}{\gamma} f_\lambda(x) = \frac{2}{\gamma}\big[x^3 - (1 - \gamma)x - \lambda\big] \,. \tag{A.18}$$

It has a local minimum at $z_0 = \sqrt{(1 - \gamma)/3}$ and a local maximum at $-z_0$. Furthermore, it is strictly increasing on $(-\infty, -z_0)$ and (z_0, ∞) and strictly decreasing on $(-z_0, z_0)$. Let $\alpha_{\min}$ and $\alpha_{\max}$ be the smallest and largest roots of $x^3 - x - \lambda$. Note that $\max\{\alpha_{\max}, -\alpha_{\min}\} = \hat{\alpha}$ and that

$$g(\alpha_{\max}) = 2\alpha_{\max} \,, \qquad g(\alpha_{\min}) = 2\alpha_{\min} \,. \tag{A.19}$$

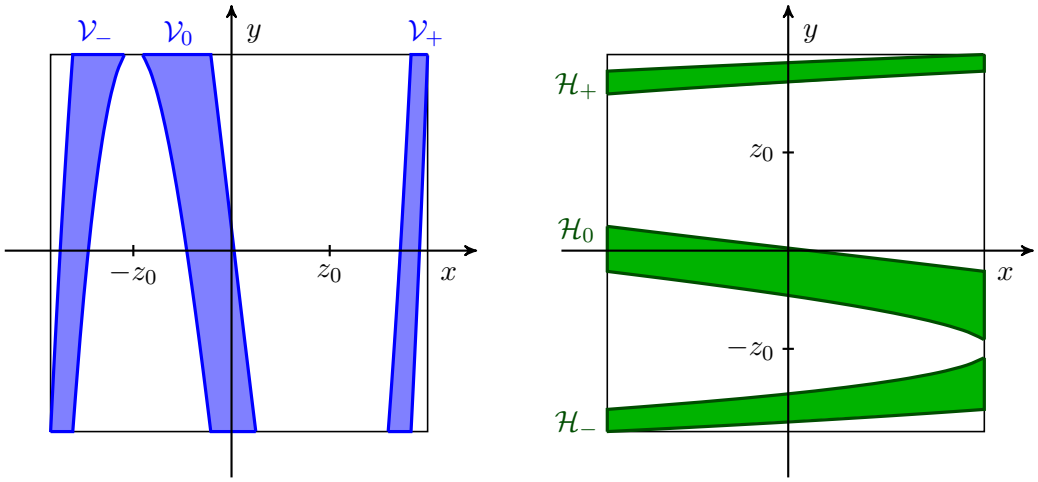

FIGURE 11. The sets $\mathcal{V}_\sigma$ and $\mathcal{H}_\sigma$ constructed in the proof of Proposition A.1. The square is the set $[\alpha_{\min}, \alpha_{\max}]^2$. The $\mathcal{V}_\sigma$ are bounded below by $g(x) - \alpha_{\max}$ and above by $g(x) - \alpha_{\min}$. Each $\mathcal{V}_\sigma$ is mapped by T to the corresponding $\mathcal{H}_\sigma$. Iterating T forward and backward in time produces an invariant Cantor set contained in the intersections of the $\mathcal{V}_\sigma$ and $\mathcal{H}_\sigma$.

Furthermore one can check that

$$(\gamma, \lambda) \in D \quad \Rightarrow \quad g(-z_0) \geqslant 2\alpha_{\max} \quad \text{and} \quad g(z_0) \leqslant 2\alpha_{\min} \,. \tag{A.20}$$

Denote by g_-^{-1} the inverse of g with range $[\alpha_{\min}, -z_0]$ and introduce the "vertical" strip

$$\mathcal{V}_- = \big\{(x,y)\colon g_-^{-1}(y+\alpha_{\min}) \leqslant x \leqslant g_-^{-1}(y+\alpha_{\max}), \alpha_{\min} \leqslant y \leqslant \alpha_{\max}\big\} \tag{A.21}$$

(see Figure 11). Then we see that T maps $\mathcal{V}_-$ to the "horizontal" strip $\mathcal{H}_- = \Pi\mathcal{V}_-$. Similarly, if g_0^{-1} denotes the inverse of g with range $[-z_0, z_0]$, then the strip

$$\mathcal{V}_0 = \big\{(x,y)\colon g_0^{-1}(y+\alpha_{\max}) \leqslant x \leqslant g_0^{-1}(y+\alpha_{\min}), \alpha_{\min} \leqslant y \leqslant \alpha_{\max}\big\} \tag{A.22}$$

is mapped by T to $\mathcal{H}_0 = \Pi\mathcal{V}_0$. In the same way, one can construct a strip $\mathcal{V}_+$ defined via the inverse g_+^{-1} of g with range $[z_0, \alpha_{\max}]$, which is mapped to $\mathcal{H}_+ = \Pi\mathcal{V}_+$. The property (A.20) ensures that the strips $\mathcal{V}_\sigma$ have disjoint interiors, and the same holds for the $\mathcal{H}_\sigma$.

Consider now any finite word $\omega = (\omega_{-n}, \ldots, \omega_{n+1}) \in \{-,0,+\}^{2(n+1)}$, and associate with it the set

$$I_\omega = \bigcap_{k=-n}^{n+1} T^k(\mathcal{V}_{\omega_k}) \,. \tag{A.23}$$

The above properties of the strips imply that all I_ω are non-empty, and have pairwise disjoint interior. In fact, the union of all I_ω converges as $n \to \infty$ to a Cantor set invariant under T. By a standard argument [24], for every doubly infinite sequence $\omega \in \{-,0,+\}^{\mathbb{Z}}$, there exists an $I_\omega \in [\alpha_{\min}, \alpha_{\max}]^2$ whose orbit visits $\mathcal{V}_{\omega_n}$ at time $-n$ and $\mathcal{H}_{\omega_n}$ at time $n+1$ for each $n \in \mathbb{N}_0$. In particular, for any of the 3^N possible N-periodic sequences ω, we obtain exactly one N-periodic orbit of T, which corresponds to one solution of (A.13). It depends continuously on the parameters γ and λ, because the I_ω depend continuously on them. □

Let us point out that the above result is consistent with the previously obtained properties of the system for $\gamma = 0$. Indeed, as $\gamma \to 0$, the function g defined in (A.18) becomes

singular, switching between $-\infty$ and $+\infty$ at the roots of $x^3 - x - \lambda$, which are precisely the α_j introduced in Section A.1. As a consequence, the invariant Cantor set collapses on $\{\alpha_0, \alpha_1, \alpha_2\}^2$, and the stationary points are all N-tuples with these coordinates (there are indeed 3^N of them).

In order to deal with the constraint $x^\star \in S$, we will need some control on the size of the sets $\mathcal{V}_\sigma \cap \mathcal{H}_{\sigma'}$. The following lemma provides upper bounds on the widths of the $\mathcal{V}_\sigma$ (and thus also on the heights of the $\mathcal{H}_{\sigma'}$) which will be sufficient for this purpose.

Lemma A.2. *Assume that $(\gamma, \lambda) \in D$, and denote by $\alpha_{\min} < \alpha_c < \alpha_{\max}$ the three roots of $x^3 - x - \lambda$. Then*

$$\begin{aligned} \mathcal{V}_- &\subset \big[\alpha_{\min}, \alpha_{\min} + \sqrt{\gamma}\,\big] \times \big[\alpha_{\min}, \alpha_{\max}\big] \,, \\ \mathcal{V}_0 &\subset \big[\alpha_c - \sqrt{\gamma}, \alpha_c + \sqrt{\gamma}\,\big] \times \big[\alpha_{\min}, \alpha_{\max}\big] \,, \\ \mathcal{V}_+ &\subset \big[\alpha_{\max} - \sqrt{\gamma}, \alpha_{\max}\big] \times \big[\alpha_{\min}, \alpha_{\max}\big] \,. \end{aligned} \tag{A.24}$$

Proof: Denote by x_1 the x-coordinate of the top-right corner of $\mathcal{V}_-$ (see Figure 11). Then we have the relations

$$\begin{aligned} x_1^3 - (1-\gamma)x_1 - \lambda &= \gamma\alpha_{\max} \,, \\ \alpha_{\min}^3 - (1-\gamma)\alpha_{\min} - \lambda &= \gamma\alpha_{\min} \,. \end{aligned} \tag{A.25}$$

Taking the difference of the two lines, writing $x_1 = \alpha_{\min} + \Delta_1$ and recalling the definition $z_0 = \sqrt{(1-\gamma)/3}$ yields

$$\Delta_1 h_1(\Delta_1) = \gamma(\alpha_{\max} - \alpha_{\min}) \,, \qquad h_1(\Delta) = 3(\alpha_{\min}^2 - z_0^2) + 3\alpha_{\min}\Delta + \Delta^2 \,. \tag{A.26}$$

One easily checks that the map $\Delta \mapsto h_1(\Delta)/\Delta$ is decreasing. Since $x_1 \leqslant -z_0$ and thus $\Delta_1 \leqslant -z_0 - \alpha_{\min}$, it follows that

$$\frac{h_1(\Delta_1)}{\Delta_1} \geqslant \frac{h_1(-z_0 - \alpha_{\min})}{-z_0 - \alpha_{\min}} = 2z_0 - \alpha_{\min} \,. \tag{A.27}$$

As a consequence, $(2z_0 - \alpha_{\min})\Delta_1^2 \leqslant \gamma(\alpha_{\max} - \alpha_{\min})$, so that we conclude that

$$\mathcal{V}_- \subset \left[\alpha_{\min}, \alpha_{\min} + \left(\frac{\gamma(\alpha_{\max} - \alpha_{\min})}{2z_0 - \alpha_{\min}}\right)^{1/2}\right] \times \big[\alpha_{\min}, \alpha_{\max}\big] \,. \tag{A.28}$$

Now we claim that $\alpha_{\max} \leqslant 2z_0$ holds for all $(\gamma, \lambda) \in D$. Indeed, if g is the function defined in (A.18), then we have by (A.14)

$$g(2z_0) = \frac{2}{\gamma}\big[\lambda_c(1-\gamma)^{3/2} - \lambda\big] \geqslant 2\hat{\alpha}(\lambda) \tag{A.29}$$

for all $(\gamma, \lambda) \in D$. Hence by (A.19) we get $g(2z_0) \geqslant 2\alpha_{\max} = g(\alpha_{\max})$, showing as claimed that $\alpha_{\max} \leqslant 2z_0$ since g is increasing on $[z_0, \infty)$. Using this bound in (A.28) yields the first relation in (A.24).

In a similar way, if x_2 denotes the x-coordinate of the top-left corner of $\mathcal{V}_0$, one obtains that $\Delta_2 = \alpha_c - x_2$ satisfies

$$\Delta_2 h_2(\Delta_2) = \gamma(\alpha_{\max} - \alpha_c) \,, \qquad h_2(\Delta) = 3(z_0^2 - \alpha_c^2) + 3\alpha_c\Delta - \Delta^2 \,. \tag{A.30}$$

One obtains again that $\Delta \mapsto h_2(\Delta)/\Delta$ is decreasing, and its smallest value, reached at $\Delta_2 = \alpha_{\rm c} + z_0$, is equal to $2z_0 - \alpha_{\rm c}$. The other relevant coordinates can be computed in the same way, yielding

$$\mathcal{V}_0 \subset \left[\alpha_{\rm c} - \left(\frac{\gamma(\alpha_{\max} - \alpha_{\rm c})}{2z_0 - \alpha_{\rm c}}\right)^{1/2}, \alpha_{\rm c} + \left(\frac{\gamma(\alpha_{\rm c} - \alpha_{\min})}{2z_0 + \alpha_{\rm c}}\right)^{1/2}\right] \times \left[\alpha_{\min}, \alpha_{\max}\right] ,$$
$$\mathcal{V}_+ \subset \left[\alpha_{\max} - \left(\frac{\gamma(\alpha_{\max} - \alpha_{\min})}{2z_0 + \alpha_{\max}}\right)^{1/2}, \alpha_{\max}\right] \times \left[\alpha_{\min}, \alpha_{\max}\right] . \tag{A.31}$$

The conclusion follows as before using $\alpha_{\max} \leqslant 2z_0$ and the symmetric relation $-\alpha_{\min} \leqslant 2z_0$. □

Fix a triple (a_0, a_1, a_2), with as usual the a_i increasing integers of sum N. We denote by λ_0 the common value of the $\alpha_j^3 - \alpha_j$, where $\{\alpha_j\}_{j\in\{0,1,2\}}$ are given in (A.3). For arbitrary $\lambda \in [-\lambda_{\rm c}, \lambda_{\rm c}]$ we define the quantity

$$\Sigma_0(\lambda) = \frac{1}{N}\big[a_0\alpha_0(\lambda) + a_1\alpha_1(\lambda) + a_2\alpha_2(\lambda)\big] , \tag{A.32}$$

where the $\alpha_j(\lambda)$ are three distinct roots of $x^3 - x - \lambda$, numbered in such a way that $\alpha_j(\lambda_0) = \alpha_j$. By construction, we have $\Sigma_0(\lambda_0) = 0$.

Proposition A.1 ensures the existence, for $(\gamma, \lambda) \in D$, of a continuous family $x^\star(\gamma, \lambda)$ of solutions of (A.13), such that $x^\star(0, \lambda)$ has a_j coordinates equal to $\alpha_j(\lambda)$. We set

$$\Sigma_\gamma(\lambda) = \frac{1}{N}\sum_{i=1}^N x_i^\star(\gamma, \lambda) . \tag{A.33}$$

It follows directly from Lemma A.2 that

$$\Sigma_0(\lambda) - \sqrt{\gamma} \leqslant \Sigma_\gamma(\lambda) \leqslant \Sigma_0(\lambda) + \sqrt{\gamma} . \tag{A.34}$$

If $\lambda \mapsto \Sigma_\gamma(\lambda)$ changes sign in D at some $\lambda_*(\gamma)$, then $x^\star(\gamma, \lambda_*(\gamma))$ is indeed a stationary point of V_γ satisfying the constraint $x^\star \in S$. Assuming for the moment that such a point exists, the following result characterises its signature.

Lemma A.3. *Assume that $(\gamma, \lambda) \in \operatorname{Int} D'$, where $D' \subset D$ is defined in* (A.15)*. Then any stationary point $x^\star$ of the family B_k, with triple $(a_0, a_1, a_2) = (0, M-k, M+k)$, is a local minimum of the constrained potential V_γ. Furthermore, there exists a constant $c_0 > 0$ such that if $\gamma \leqslant c_0\sqrt{\lambda_c - |\lambda|}$, then any stationary point $x^\star$ of the family C_k, with triple $(a_0, a_1, a_2) = (1, M-k-1, M+k)$, is a saddle of index 1 of the constrained potential V_γ.*

Proof: First we note that by definition of D', the function g defined in (A.18) satisfies

$$g\left(-\frac{1}{\sqrt{3}}\right) = \frac{2}{\gamma}(\lambda_{\rm c} - \lambda) - \frac{2}{\sqrt{3}} > \frac{4}{\sqrt{3}} \geqslant 2\alpha_{\max} , \tag{A.35}$$

which implies that points in $\mathcal{V}_-$ have a first coordinate x satisfying $x < -1/\sqrt{3}$, and thus $3x^2 > 1$. By symmetry, points in $\mathcal{V}_+$ also have a first coordinate satisfying $3x^2 > 1$. Stationary points $x^\star$ in the family B_k have all coordinates in $\mathcal{V}_\pm$, since they are deformations of points with all coordinates equal to $\alpha_{\min}$ or $\alpha_{\max}$. The Hessian matrix H_γ of the unconstrained potential at any stationary point $x^\star$ defines the quadratic form

$$v \mapsto \langle v, H_\gamma v\rangle = \sum_{i=1}^N \big(3(x^\star)^2 - 1\big)v_i^2 + \frac{\gamma}{2}\sum_{i=1}^N \big(v_i - v_{i+1}\big)^2 . \tag{A.36}$$

This form is clearly positive definite if $x^\star \in B_k$, showing that $x^\star$ is a local minimum of the unconstrained potential. Thus it is also a local minimum of the constrained potential.

In the case where $x^\star \in C_k$, it has exactly one coordinate x in $\mathcal{V}_0$, for which one easily checks that $3x^2 < 1$. Thus H_0 has exactly one negative eigenvalue, showing that for $\gamma = 0$, $x^\star$ is a 1-saddle of the unconstrained potential. By Proposition 3.1, $x^\star$ is also a 1-saddle of the constrained potential, so that there exists a vector $v \in S$ such that $\langle v, H_0 v\rangle < 0$. In fact, one can deduce from (A.8) that the negative eigenvalue of H_0 is bounded above by $-c_1\sqrt{\lambda_c - |\lambda|}$ for a $c_1 > 0$, while its other eigenvalues are bounded below by $c_1\sqrt{\lambda_c - |\lambda|}$. Since the second term in (A.36) has an ℓ^2-operator norm equal to γ (it is a discrete Laplacian, diagonalisable by discrete Fourier transform), the Bauer–Fike theorem shows that $x^\star$ remains a 1-saddle of the unconstrained potential as long as $\gamma < c_2\sqrt{\lambda_c - |\lambda|}$ for some $c_2 > 0$.

To show that this also holds for the constrained potential, we can use the fact that the eigenvectors of a perturbed matrix move by an amount controlled by the size of the perturbation (see for instance [13, Thm. 4.1]). In this way, we obtain the existence of an orthogonal matrix O_γ such that $\delta O_\gamma = O_\gamma - \mathbb{1}$ has order $\gamma/\sqrt{\lambda_c - |\lambda|}$ and $D_\gamma = O_\gamma H_\gamma O_\gamma^{\mathrm{T}}$ is diagonal, with the same eigenvalues as H_γ. It follows by Cauchy–Schwarz that

$$\begin{aligned}\langle v, H_\gamma v\rangle &= \langle O_\gamma v, D_\gamma O_\gamma v\rangle \\ &= \langle v, D_\gamma v\rangle + 2\langle \delta O_\gamma v, D_\gamma v\rangle + \langle \delta O_\gamma v, D_\gamma \delta O_\gamma v\rangle \\ &\leqslant \left(-c_3\sqrt{\lambda_c - |\lambda|} + \frac{c_4\gamma}{\sqrt{\lambda_c - |\lambda|}} + \frac{c_5\gamma^2}{\lambda_c - |\lambda|}\right)\|v\|^2 \end{aligned} \tag{A.37}$$

for constants $c_3, c_4, c_5 > 0$. This shows that for $\gamma/(\lambda_c - |\lambda|)$ sufficiently small, $\langle v, H_\gamma v\rangle < 0$ and thus $x^\star$ is a saddle of index at least 1 of the constrained system. However, the index cannot be larger than for the unconstrained system, so that if must equal 1. □

Proof of Theorem 3.6. If we denote by $\pm\hat{\lambda}(\gamma)$ the upper and lower boundaries of D, then a sufficient condition for Σ_γ to change sign is

$$\Sigma_0(\hat{\lambda}(\gamma)) > \sqrt{\gamma} \qquad \text{and} \qquad \Sigma_0(-\hat{\lambda}(\gamma)) < -\sqrt{\gamma}\,. \tag{A.38}$$

Without limiting the generality, we assume $\lambda_0 \geqslant 0$. Then the first of the two conditions is the more stringent one. For the family B_k, using the fact that $\alpha_{\min}(\lambda) = -\frac{1}{\sqrt{3}} - \mathcal{O}(\sqrt{\lambda_c - \lambda}\,)$ near λ_c we obtain

$$\Sigma_0(\lambda) = \frac{1}{\sqrt{3}}\left(\frac{1}{2} - \frac{3k}{N}\right) - c\left(\frac{1}{2} + \frac{k}{N}\right)\sqrt{\lambda_c - \lambda} + \mathcal{O}(\lambda_c - \lambda) \tag{A.39}$$

for some constant $c > 0$. Since we also have $\hat{\lambda}(\gamma) \geqslant \lambda_c(1 - \frac{9}{2}\gamma) = \lambda_c - \sqrt{3}\gamma$, inserting this in (A.38) yields the result. The case of the families C_k is similar, noting that the bound on γ in Lemma A.3 ensuring that they remain 1-saddles is fulfilled under the condition (3.6).

In the case of the family B_0, one can obtain sharper bounds by first noting that $x^\star$ has exactly half of its components in $\mathcal{V}_-$ and the other half in $\mathcal{V}_+$. Using the bounds given in Lemma A.2, we see that (A.34) can be strengthened to

$$\Sigma_0(\lambda) - \frac{1}{2}\sqrt{\gamma} \leqslant \Sigma_\gamma(\lambda) \leqslant \Sigma_0(\lambda) + \frac{1}{2}\sqrt{\gamma}\,. \tag{A.40}$$

Furthermore, we have

$$\Sigma_0(\lambda) = \frac{1}{2}\alpha_{\min}(\lambda) + \frac{1}{2}\alpha_{\max}(\lambda) = -\frac{1}{2}\alpha_c(\lambda)\,. \tag{A.41}$$

A sufficient condition for the stationary point to exist is thus

$$-\alpha_{\mathrm{c}}\big(\lambda_{\mathrm{c}}(1-\tfrac{9}{2}\gamma)\big) > \sqrt{\gamma}\,. \tag{A.42}$$

By definition of α_{c}, this is equivalent to $\lambda_{\mathrm{c}}(1-\frac{9}{2}\gamma) > \sqrt{\gamma}(\gamma-1)$. Taking the square yields the condition $27\gamma^3 - 135\gamma^2 + 54\gamma - 4 < 0$, which holds for $\gamma < \frac{7}{3} - \sqrt{5}$. □

B Proofs: Metastable hierarchy

B.1 Hierarchy of the B_k

Proof of Theorem 4.4. When $\gamma = 0$, the value of the potential is constant on each family B_k and C_k. Using the expressions (A.3) of the α_j, one obtains for these values

$$V_0(B_k) = -\frac{aN(N-a)}{4(N^2-3aN+3a^2)}\,, \qquad V_0(C_{k+1}) = -\frac{aN^2-(a^2+8a-8)N+9a(a-1)}{4(N^2-3aN+3a^2-3a+3)}\,, \tag{B.1}$$

where $a = M - k$ in both cases. Taking differences and simplifying yields

$$V_0(C_{k+1}) - V_0(B_k) = \frac{(a-1)(2N-3a)^3}{4(N^2-3aN+3a^2)(N^2-3aN+3a^2-3a+3)} =: h_1(a)\,, \tag{B.2}$$
$$V_0(C_k) - V_0(B_k) = \frac{(N-a-1)(3a-N)^3}{4(N^2-3aN+3a^2)(N^2-3(a+1)N+3a^2+3a+3)} =: h_2(a)\,.$$

Computing derivatives and proceeding in a similar way as in the proof of Theorem 3.5, one obtains that $a \mapsto h_1(a)$ is decreasing, while $a \mapsto h_2(a)$ is increasing. Furthermore, it is immediate to check that $h_1(N/2) = h_2(N/2)$. We thus obtain the inequalities

$$\cdots < V_0(C_2) - V_0(B_2) < V_0(C_1) - V_0(B_1) < V_0(C_1) - V_0(B_0) < V_0(C_2) - V_0(B_1) < \dots \tag{B.3}$$

(cf. Figure 6). To prove (4.6), we have to check that relation (4.2) holds for each B_k. Indeed, on the one hand we have

$$H\Big(B_k, \bigcup_{i=0}^{k-1} B_i\Big) = V_0(C_k) - V_0(B_k) \tag{B.4}$$

for $k \geqslant 2$, while on the other hand

$$H\Big(B_\ell, \bigcup_{i=0}^{k} B_i \setminus B_\ell\Big) \geqslant V_0(C_\ell) - V_0(B_\ell)\,, \qquad \ell \in [\![2, k-1]\!]\,,$$
$$H\Big(B_0, \bigcup_{i=1}^{k} B_i\Big) = V_0(C_1) - V_0(B_0)\,. \tag{B.5}$$

Thus the result follows from (B.3).

When $\gamma > 0$ is sufficiently small, the same partition still forms a metastable hierarchy, because the potential heights of the critical points depend continuously on γ. □

B.2 Hierarchy on B_0

Proof of Proposition 4.7. The fact that allowed transitions between elements in B_0 correspond to exchanging a particle and a hole follow directly from the connection rules (3.5). Indeed, any element in B_1, with triple $(0, M-1, M+1)$, is connected to $M+1$ elements of B_0, which differ by a particle/hole transposition (see also Figure 4). Any such transition affects at most 4 interfaces. Since the number of interface is always even, we obtain (4.12).

In order to compute communication heights, we have to determine the heights of 1-saddles $z^\star$ in C_1. Recall that each of these saddles has 1 coordinate equal to α'_0, $M-1$ coordinates equal to α'_1 and M coordinates equal to α'_2, where

$$(\alpha'_0, \alpha'_1, \alpha'_2) = \pm\omega'(1, 1-M, M-2) \;, \qquad \omega' = (M^2-3M+3)^{-1/2} \;. \tag{B.6}$$

Plugging this into (4.10) yields

$$\begin{aligned} V_\gamma\big(z^\star(\gamma)\big) = V_0\big(z^\star(0)\big) \\ &+ \frac{\gamma}{4}(\omega')^2\big[M^2 I_{\alpha'_0/\alpha'_1}(z^\star) + (M-3)^2 I_{\alpha'_0/\alpha'_2}(z^\star) + (2M-3)^2 I_{\alpha'_1/\alpha'_2}(z^\star)\big] \\ &+ \mathcal{O}(\gamma^2) \;, \end{aligned} \tag{B.7}$$

where, similarly to (4.9), $I_{\alpha'_i/\alpha'_j}(z^\star)$ denotes the number of interfaces of type α'_i/α'_j of $z^\star$. The first-order correction to the height of the saddle thus only depends on the triple

$$I(z^\star) = \big[I_{\alpha'_0/\alpha'_1}(z^\star), I_{\alpha'_0/\alpha'_2}(z^\star), I_{\alpha'_1/\alpha'_2}(z^\star)\big] \;, \tag{B.8}$$

where we use square brackets in order to avoid confusion with the triple $(0, M-1, M+1)$. Note in particular that $I_{\alpha'_0/\alpha'_1}(z^\star) + I_{\alpha'_0/\alpha'_2}(z^\star) = 2$, since only 1 component of $z^\star$ is equal to α'_0. The following lemma allows to compare all these saddle heights.

Lemma B.1. *For all even $p \in [\![2, N-2]\!]$, the first-order terms $V^{(1)}$ in* (B.7) *satisfy*

$$V^{(1)}\big([2,0,p]\big) > V^{(1)}\big([0,2,p]\big) > V^{(1)}\big([1,1,p-1]\big) > V^{(1)}\big([2,0,p-2]\big) \;, \tag{B.9}$$

where $[a,b,c]$ stands for any saddle $z^\star$ such that $I(z^\star) = [a,b,c]$.

Proof: This follows from a straightforward computation, using (B.7) and the fact that $(2M-3)(M-3) > 0$. □

It remains to apply these expressions to the different transitions in Table 1. Consider for instance the transition shown in Figure 4, which is of type II.b. The two saddles encountered during the transition are of type $[1,1,p-1]$ and $[0,2,p]$, where $p=2$ is the number of interfaces of the start configuration $x^\star$. Lemma B.1 shows that the second saddle is the highest. Combining this with the expression (4.10) of the height of $x^\star$ yields

$$H^{(1)} = \frac{2(M-3)^2 + p(2M-3)^2}{4(M^2-3M+3)} - p = \frac{2(M-3)^2 - 3p}{4(M^2-3M+3)} \;, \tag{B.10}$$

which is precisely the expression given in the second line of Table 1.

The other cases are treated in a similar way. One just has to take care of the fact that the transition rules (3.5) allow for two possible paths, depending on whether $(\alpha_1, \alpha_2) = (1,-1) + \mathcal{O}(\gamma)$ or $(-1,1) + \mathcal{O}(\gamma)$. It is thus necessary to determine the minimum of the communication heights associated with these two paths. Table 2 shows the associated saddles in cases where the exchanged sites are not nearest neighbours. Table 3 shows the same when the exchanged sites are nearest neighbours. These saddle interface numbers are indeed those shown in Table 1. □

	I	II.a/b	III	IV.a/b	V.a/b	VI
η	$(0,0)$	$(0,1)/(1,0)$	$(1,1)$	$(0,2)/(2,0)$	$(1,2)/(2,1)$	$(2,2)$
$I(z^\star)$	$[0,2,p+2]$	$[0,2,p]$	$[1,1,p-1]$	$[0,2,p-2]$	$[0,2,p-2]$	$[0,2,p-2]$

TABLE 2. Interface numbers of the highest saddle encountered along a minimal path between two configurations in B_0, if the two exchanged sites i and j are not nearest neighbours. The labels in the first row are the same as in Table 1, and η denotes the number of interfaces of i and j.

	II.c	IV.c/d	V.c
η	$(1,1)$	$(1,2)/(2,1)$	$(2,2)$
$I(z^\star)$	$[0,2,p]$	$[0,2,p-2]$	$[0,2,p-2]$

TABLE 3. Interface numbers of the highest saddle encountered along a minimal path between two configurations in B_0, if the two exchanged sites i and j are nearest neighbours.

Proof of Theorem 4.8. In a similar way as in the proof of Theorem 4.4, we prove that the relation (4.2) holds when the A_p and A'_p are ordered according to (4.15). Since all communication heights are the same when $\gamma = 0$, it will be sufficient to compare the first-order coefficients $H^{(1)}$.

We start by showing that $A_2 \prec A'_4 \prec \cdots \prec A'_{M'}$. For any $p \in [\![4, M']\!]$, we note that

$$H^{(1)}(A'_p, A_2 \cup A'_4 \cup \cdots \cup A'_{p-2}) = H^{(1)}(A'_p, A_p) = \frac{-2M^2 + 6M - 3p}{4(M^2 - 3M + 3)} \,. \tag{B.11}$$

Indeed, the highest saddle encountered along a minimal path from A'_p to $A_2 \cup A'_4 \cup \ldots A'_{p-2}$ occurs during the type-III transition from A'_p to A_p, and has interface number $[1, 1, p-1]$. Since (B.11) is a decreasing function of p, the condition (4.2) is indeed satisfied.

Next we observe that

$$H^{(1)}(A_4, A_2 \cup A'_4 \cup \cdots \cup A'_{M'}) = H^{(1)}(A_4, A_2) = \frac{-6M^2 + 12M - 12}{4(M^2 - 3M + 3)} \,. \tag{B.12}$$

Indeed, here the minimal path goes directly from A_4 to A_2, via a saddle of type $[0, 2, 2]$. The expression (B.12) is indeed smaller than (B.11) for $p = M'$, the numerator of the difference being bounded by $4M^2 - 9M + 12$ which is always positive.

Finally, we see that we have

$$H^{(1)}(A_p, A_2 \cup \cdots \cup A'_{M'} \cup A_4 \cup \cdots \cup A_{p-2}) = H^{(1)}(A_p, A_{p-2}) = \frac{-6M^2 + 12M - 3p}{4(M^2 - 3M + 3)} \,, \tag{B.13}$$

the minimal path reaching communication height on a saddle of type $[0, 2, p-2]$. Since (B.13) is again a decreasing function of p, the claim follows. □

C Proofs: Spectral gap

In order to prove Theorem 5.1, we have to take into account the symmetries of the potential V_γ. This will allow us to apply the theory in [5] on metastable processes that are invariant under a group of symmetries, which relies on Frobenius' representation theory of finite groups (see for instance [30]).

The potential V_γ is invariant under the three transformations

$$\begin{aligned} r &: (x_1, \dots, x_N) \mapsto (x_2, \dots, x_N, x_1) \ , \\ s &: (x_1, \dots, x_N) \mapsto (x_N, \dots, x_1) \ , \\ c &: (x_1, \dots, x_N) \mapsto (-x_1, \dots, -x_N) \ . \end{aligned} \tag{C.1}$$

It is thus invariant under the group G generated by these three transformations. This group can be written $G = \mathfrak{D}_N \times \mathbb{Z}_2$, where $\mathfrak{D}_N$ is the dihedral group of symmetries of a regular N-gon generated by r and s, while $\mathbb{Z}_2 = \{\mathrm{id}, c\}$ is the group generated by c, which commutes with r and s. The group G has order $4N$, and its elements can be written $r^i s^j c^k$ with $i \in [\![0, N-1]\!]$ and $j, k \in \{0, 1\}$. It admits exactly 8 one-dimensional irreducible representations given by

$$\pi_{\rho\sigma\tau}(r^i s^j c^k) = \rho^i \sigma^j \tau^k \ , \qquad \rho, \sigma, \tau = \pm 1 \ , \tag{C.2}$$

and $N - 2$ irreducible representation of dimension 2, whose characters are

$$\chi_{\ell,\pm}(r^i s^j c^k) = \operatorname{Tr} \pi_{\ell,\pm}(r^i s^j c^k) = 2 \cos\left(\frac{2i\ell\pi}{N}\right) \delta_{j0} (\pm 1)^k \ , \qquad \ell \in [\![1, \tfrac{N}{2} - 1]\!] \ . \tag{C.3}$$

The basic idea of the approach given in [5] is that each of these $N + 6$ irreducible representations provides an invariant subspace of the generator L of the Markovian jump process on $\mathcal{S}_0$ that approximates the dynamics of the diffusion. Thus the restriction of L to each of these subspaces yields a part of the spectrum of L. The eigenvalues of L can then be shown to be close to the exponentially small eigenvalues of $\mathcal{L}$ [17, 16]. We thus have to determine, for each irreducible representation, the smallest eigenvalue of $-L$. We do this in two main steps: first we show that the Arrhenius exponent of each smallest nonzero eigenvalue is given by the potential difference between certain stationary points in C_1 and in A_2, and then we compute the smallest prefactor of these eigenvalues.

C.1 Arrhenius exponent

Each $g \in G$ induces a permutation π_g on the set of local minima $\mathcal{S}_0$, leaving invariant each group orbit $O_a = \{ga \colon g \in G\}$. Since V_γ is G-invariant, the generator L commutes with all these permutations. Thus there exist subspaces which are jointly invariant under L and all the π_g. Each of the irreducible representations of G provides one of these subspaces.

Let π be one of the irreducible representations of G, and let $d \in \{1, 2\}$ be its dimension. Then [5, Lemma 3.6] shows that the associated invariant subspace, when restricted to O_a, has dimension $d\alpha_a^\pi$, where

$$\alpha_a^\pi = \frac{1}{|G_a|} \sum_{h \in G_a} \chi(h) \in [\![0, d]\!] \ . \tag{C.4}$$

Here $\chi = \operatorname{Tr} \pi$ denotes the character of π, and $G_a = \{g \in G \colon ga = a\}$ the stabiliser of a. We call *active* with respect to the irreducible representation π the orbits O_a such that $\alpha_a^\pi > 0$. Only active orbits will occur in the restriction of L to the invariant subspace associated with π; they are represented by a block of size $d\alpha_a^\pi \times d\alpha_a^\pi$.

We select three representatives $x^\star \in A_2$, $y^\star \in B_1$ and $z^\star \in C_1$ such that $x^\star$ is connected to $y^\star$ via $z^\star$ in the transition graph $\mathcal{G}$. A possible choice is

$$\begin{aligned} x^\star &= (\alpha_1, \dots, \alpha_1, \alpha_1, \alpha_2 \dots, \alpha_2) \ , \\ z^\star &= (\alpha_1', \dots, \alpha_1', \alpha_0', \alpha_2' \dots, \alpha_2') \ , \\ y^\star &= (\alpha_1'', \dots, \alpha_1'', \alpha_2'', \alpha_2'' \dots, \alpha_2'') \ , \end{aligned} \tag{C.5}$$

where $\alpha_1 = 1 + \mathcal{O}(\gamma)$, $\alpha_2 = -1 + \mathcal{O}(\gamma)$ and α_2' are each repeated M times, α_1' and α_1'' are repeated $M-1$ times and α_2'' is repeated $M+1$ times. The orbit O_x of $x^\star$ is precisely A_2, and it has N elements. The orbits O_y of $y^\star$ and O_z of $z^\star$ have respectively $2N$ and $4N$ elements (they are proper subsets of B_1 and C_1). The associated stabilisers are given by

$$\begin{aligned} G_x &= \{\mathrm{id}, r^M s, r^M c, sc\} \,, \\ G_y &= \{\mathrm{id}, r^{M-1} s\} \,, \\ G_z &= \{\mathrm{id}\} \,, \end{aligned} \tag{C.6}$$

where id denotes the identity of G and $M = \frac{N}{2}$. Note in particular that

$$\frac{|G_x|}{|G_x \cap G_y|} = 4 \,, \qquad \frac{|G_y|}{|G_x \cap G_y|} = 2 \,. \tag{C.7}$$

This means that each element in G_x is connected to 4 elements in G_y (via 4 saddles in G_z), and that each element in G_y is connected to 2 elements in G_x (cf. [5, (2.25)]).

The possible Arrhenius exponents of eigenvalues of L are directly linked to which orbits are active for the different irreducible representations. We start with irreducible representations of dimension 1, cf. (C.2).

Proposition C.1. *Let π be a 1-dimensional irreducible representation of G. Then*

- *if M is even, then $O_x = A_2$ is active if and only if $\pi(s) = \pi(c) = 1$;*
- *if M is odd, then $O_x = A_2$ is active if and only if $\pi(r) = \pi(s) = \pi(c)$;*
- *if M is even, then O_y is active if and only if $\pi(r) = \pi(s)$;*
- *if M is odd, then O_y is active if and only if $\pi(s) = 1$.*

Proof: The orbit O_x is active if and only if $\pi(g) = 1$ for all $g \in G_x$. Since $\pi(\mathrm{id}) = 1$, $\pi(r^M s) = \pi(r)^M \pi(s)$, $\pi(r^M c) = \pi(r)^M \pi(c)$ and $\pi(sc) = \pi(s)\pi(c)$, this holds if and only if $\pi(r)^M = \pi(s) = \pi(c)$. Similarly, the orbit O_y is active if and only if $\pi(r)^{M-1} = \pi(s)$. □

The corresponding result for the 2-dimensional irreducible representations given in (C.3) reads as follows.

Proposition C.2. *Let $\pi_{\ell,\pm}$ be a 2-dimensional irreducible representation. Then*

- *$O_x = A_2$ is active for $\pi_{\ell,+}$ if and only if ℓ is even;*
- *$O_x = A_2$ is active for $\pi_{\ell,-}$ if and only if ℓ is odd;*
- *O_y is active for all representations $\pi_{\ell,\pm}$.*

Proof: By (C.3) we have $\chi_{\ell,\pm}(\mathrm{id}) = 2$, $\chi_{\ell,\pm}(r^M s) = 0$, $\chi_{\ell,\pm}(r^M c) = \pm 2\cos(\ell\pi)$ and $\chi_{\ell,\pm}(sc) = 0$. Thus the sum (C.4) for O_x is different from 0 for $\chi_{\ell,+}$ if and only if ℓ is even, and for $\chi_{\ell,-}$ if and only if ℓ is odd. Since $\chi_{\ell,\pm}(r^{M-1}s) = 0$, the sum for O_y is always equal to 1. □

Corollary C.3. *The maximal Arrhenius exponent of all nonzero eigenvalues of the generator is given by $V_\gamma(z^\star) - V_\gamma(x^\star)$.*

Proof: [5, Thm. 3.5] provides an algorithm determining the Arrhenius exponents for each irreducible representation π of dimension 1. They are obtained by replacing all inactive orbits by a cemetery state, which is at the bottom of the metastable hierarchy, and ordering all other orbits according to the usual hierarchy. If $O_x = A_2$ is active and O_y is inactive for π, then the largest communication height determining an Arrhenius exponent will be given

by $V_\gamma(z^\star) - V_\gamma(x^\star)$. If M is even, the representation π_{-++} has the required property, while if M is odd, this rôle is played by π_{---}.

In the case of 2-dimensional representations, [5, Thm. 3.9] shows that all communication heights between active orbits yield Arrhenius exponents. The largest such exponent is obtained if O_x and O_y are both active, and Proposition C.2 shows that there are representations for which this is the case. □

C.2 Eyring–Kramers prefactor

It remains to find the smallest prefactor associated with a transition of communication height $V_\gamma(z^\star) - V_\gamma(x^\star)$. In the case of one-dimensional representations, [5, Prop. 3.4] shows that the usual Eyring–Kramers law given in Theorem 4.3 has to be corrected by a factor $|G_x|/|G_x \cap G_y| = 4$ (cf. (C.7)).

In the case of two-dimensional irreducible representations $\pi_{\ell,\pm}$, the relevant matrix elements are given in [5, Prop. 3.7]. Alternatively, one can compute these elements "by hand" in the following way. We start by ordering the elements of the two orbits O_x and O_y according to

$$\begin{aligned} O_x &= \{x^\star, rx^\star, \dots, r^{N-1}x^\star\} , \\ O_y &= \{y^\star, ry^\star, \dots, r^{N-1}y^\star, r^M cy^\star, r^{M+1}cy^\star, \dots, r^{M-1}cy^\star\} . \end{aligned} \tag{C.8}$$

The restriction of L to $O_x \cup O_y$ consists in the four blocks

$$L_{xx} = -4q_x \mathbb{1}_N , \qquad L_{yy} = -2q_y \mathbb{1}_{2N} ,$$

$$L_{xy} = q_x \begin{pmatrix} 1 & 1 & & (0) & 1 & 1 & & (0) \\ & \ddots & \ddots & & & \ddots & \ddots & \\ & (0) & \ddots & 1 & & (0) & \ddots & 1 \\ 1 & & & 1 & 1 & & & 1 \end{pmatrix} , \quad L_{yx} = q_y \begin{pmatrix} 1 & & & 1 \\ 1 & \ddots & (0) & \\ & \ddots & \ddots & \\ (0) & & 1 & 1 \\ 1 & & & 1 \\ 1 & \ddots & (0) & \\ & \ddots & \ddots & \\ (0) & & 1 & 1 \end{pmatrix} , \tag{C.9}$$

where $\mathbb{1}_n$ denotes the $n \times n$ identity matrix, (0) stands for repeated zero entries, and

$$q_x = \frac{|\lambda_-(z^\star)|}{2\pi} \sqrt{\frac{\det \nabla^2 V_\gamma(x^\star)}{\det \nabla^2 V_\gamma(z^\star)}}\, \mathrm{e}^{-[V_\gamma(z^\star) - V_\gamma(x^\star)]/\varepsilon} \big[1 + \mathcal{O}(\varepsilon^{1/2} |\log \varepsilon|^{3/2})\big] , \tag{C.10}$$

while q_y is a positive constant of order $\mathrm{e}^{-[V_\gamma(z^\star) - V_\gamma(y^\star)]/\varepsilon}$. Equation (3.14) in [5] provides a set of vectors spanning the invariant subspaces associated with a given irreducible representation. Among these, we have to choose two linearly independent vectors for each orbit. A possible choice is

$$\begin{aligned} u^x &= (2, \chi(r), \dots, \chi(r^{N-1}), 0, \dots, 0) , \\ u^{rx} &= (\chi(r^{N-1}), 2, \chi(r), \dots, \chi(r^{N-2}), 0, \dots, 0) , \\ u^y &= (0, \dots, 0, 2, \chi(r), \dots, \chi(r^{N-1}), 2, \chi(r), \dots, \chi(r^{N-1})) , \\ u^{ry} &= (0, \dots, 0, \chi(r^{N-1}), 2, \chi(r), \dots, \chi(r^{N-2}), \chi(r^{N-1}), 2, \chi(r), \dots, \chi(r^{N-2})) , \end{aligned} \tag{C.11}$$

where $\chi = \chi_{\ell,\pm}$ is given by (C.3). In this basis, L takes the block form

$$L^\pi_{xx} = -q_x \begin{pmatrix} 4 & 0 \\ 0 & 4 \end{pmatrix} , \qquad L^\pi_{yy} = -q_y \begin{pmatrix} 2 & 0 \\ 0 & 2 \end{pmatrix} ,$$
$$L^\pi_{xy} = q_x \begin{pmatrix} 2(\chi(r)+1) & 2 \\ -2 & 2 \end{pmatrix} , \qquad L^\pi_{yx} = q_y \begin{pmatrix} 1 & -1 \\ 1 & (\chi(r)+1) \end{pmatrix} . \tag{C.12}$$

We can now apply [5, Thm. 3.9], which states that the eigenvalues are equal to those of

$$L^\pi_{xx} - L^\pi_{xy}\big(L^\pi_{yy}\big)^{-1} L^\pi_{yx} = -4\sin^2\left(\frac{\ell\pi}{N}\right) q_x \mathbb{1}_2 . \tag{C.13}$$

The result (5.1) follows, since the minimal value of the eigenvalues is reached for $\ell = 1$, both orbits are active for the representation $\pi_{1,-}$, and this value is smaller than for all one-dimensional representations.

Remark C.4. It is of course possible to obtain the same result directly from the expressions (3.15) and (3.17) given in [5] for the inner products $\langle u, Lv\rangle$, where u and v are basis vectors among (C.11), even though these vectors are not orthogonal. It suffices to use the fact that the matrix elements of L can be obtained by computing

$$\begin{pmatrix} 1 & \dfrac{\langle u,v\rangle}{\langle u,u\rangle} \\ \dfrac{\langle u,v\rangle}{\langle v,v\rangle} & 1 \end{pmatrix}^{-1} \begin{pmatrix} \dfrac{\langle u,Lu\rangle}{\langle u,u\rangle} & \dfrac{\langle u,Lv\rangle}{\langle u,u\rangle} \\ \dfrac{\langle v,Lu\rangle}{\langle v,v\rangle} & \dfrac{\langle v,Lv\rangle}{\langle v,v\rangle} \end{pmatrix} \tag{C.14}$$

where for instance $\langle u^x, u^{rx}\rangle = \cos(\ell\pi/M)\langle u^x, u^x\rangle$. $\Diamond$

The last element of the proof of Theorem 5.1 is the following result on the Hessian matrices of V_0.

Proposition C.5. *The Hessian matrices of V_0 at $x^\star$ and $z^\star$ satisfy*

$$\det \nabla^2 V_0(x^\star) = 2^{N-1} ,$$
$$\det \nabla^2 V_0(z^\star) = -\frac{M^{M-2}(M-3)^M(2M-3)^{2M-2}}{(M^2-3M+3)^{2M-2}} = -2^{N-2}\big[1+\mathcal{O}(N^{-1})\big] ,$$
$$\lambda_-(z^\star) = -\frac{(M-3)(2M-3)}{2(M^2-3M+3)} = -1+\mathcal{O}(N^{-1}) . \tag{C.15}$$

Proof: We have already obtained invariant subspaces of the Hessian matrices in the proof of Proposition 3.1. However, since we used a non-isometric parametrisation of S, we cannot use expressions such as (A.7) directly to determine the eigenvalues.

In the case of $x^\star = (1,\dots,1,-1,\dots,-1)$, it is sufficient to note that for any vector u of unit length in S, one has

$$\frac{\mathrm{d}^2}{\mathrm{d}t^2} V_0(x^\star + tu)\Big|_{t=0} = \sum_{i=1}^{M} u_i^2 U''(1) + \sum_{i=M+1}^{N} u_i^2 U''(-1) = 2 , \tag{C.16}$$

showing that in fact $\nabla^2 V_0(x^\star) = 2\mathbb{1}_{N-1}$, which has determinant 2^{N-1}.

In the case of the saddle $z^\star$ given by (C.5), the expressions (A.3) for the α'_j yield

$$\begin{aligned} U''(\alpha'_0) = 3(\alpha'_0)^2 - 1 = -\frac{M(M-3)}{M^2-3M+3} &= -1 + \mathcal{O}(M^{-2}) \,, \\ U''(\alpha'_1) = 3(\alpha'_1)^2 - 1 = \frac{M(2M-3)}{M^2-3M+3} &= 2 + 3M^{-1} + \mathcal{O}(M^{-2}) \,, \\ U''(\alpha'_2) = 3(\alpha'_2)^2 - 1 = \frac{(M-3)(2M-3)}{M^2-3M+3} &= 2 - 3M^{-1} + \mathcal{O}(M^{-2}) \,. \end{aligned} \tag{C.17}$$

We know from the proof of Proposition 3.1 that the $(M-2)$-dimensional subspace of S given by $S_1 = \{x_1 + \cdots + x_{M-1} = 0, x_M = \cdots = x_N = 0\}$ is invariant by the Hessian. Proceeding as in (C.16) with a unit vector $u \in S_1$ shows that $U''(\alpha'_1)$ is an eigenvalue of $\nabla^2 V_0(z^\star)$ of multiplicity $M-2$. In an analogous way, the $(M-1)$-dimensional invariant subspace of S given by $S_2 = \{x_1 = \cdots = x_M = 0, x_{M+1} + \cdots + x_N = 0\}$ carries the eigenvalue $U''(\alpha'_2)$ with a multiplicity $M-1$. This leaves a two-dimensional invariant subspace, for which we may choose the orthonormal basis given by the vectors

$$\begin{aligned} \hat{v} &= \tfrac{1}{\sqrt{2M}}(1, \dots, 1, 1, -1, \dots, -1) \,, \\ \hat{w} &= \tfrac{1}{\sqrt{M(M-1)}}(-1, \dots, -1, M-1, 0, \dots, 0) \,. \end{aligned} \tag{C.18}$$

The Hessian at $(0,0)$ of the map $(t,s) \mapsto V_0(z^\star + t\hat{v} + s\hat{w})$ is found to be the matrix

$$\frac{1}{2(M^2-3M+3)} \begin{pmatrix} 4M^2-15M+15 & -3\sqrt{2(M-1)}(M-2) \\ -3\sqrt{2(M-1)}(M-2) & -2(M^2-6M+6) \end{pmatrix} \,, \tag{C.19}$$

which has eigenvalues

$$2 \qquad \text{and} \qquad -\frac{(M-3)(2M-3)}{2(M^2-3M+3)} = -1 + \mathcal{O}(N^{-1}) \,. \tag{C.20}$$

The result follows via a Taylor expansion of $\log(-\det \nabla^2 V_0(z^\star))$. □

References

[1] D. C. Antonopoulou, P. W. Bates, D. Blömker, and G. D. Karali. Motion of a droplet for the mass-conserving stochastic Allen–Cahn equation. Preprint `arXiv:1501.05288`.

[2] F. Barret. Sharp asymptotics of metastable transition times for one dimensional SPDEs. *Ann. Inst. Henri Poincaré Probab. Stat.*, 51(1):129–166, 2015.

[3] F. Barret, A. Bovier, and S. Méléard. Uniform estimates for metastable transition times in a coupled bistable system. *Electron. J. Probab.*, 15:no. 12, 323–345, 2010.

[4] N. Berglund. Kramers' law: Validity, derivations and generalisations. *Markov Process. Related Fields*, 19(3):459–490, 2013.

[5] N. Berglund and S. Dutercq. The Eyring–Kramers law for Markovian jump processes with symmetries. *Journal of Theoretical Probability*, Online First:1–40, 2015.

[6] N. Berglund, B. Fernandez, and B. Gentz. Metastability in interacting nonlinear stochastic differential equations I: From weak coupling to synchronization. *Nonlinearity*, 20(11):2551–2581, 2007.

[7] N. Berglund, B. Fernandez, and B. Gentz. Metastability in interacting nonlinear stochastic differential equations II: Large-N behaviour. *Nonlinearity*, 20(11):2583–2614, 2007.

[8] N. Berglund and B. Gentz. The Eyring–Kramers law for potentials with nonquadratic saddles. *Markov Processes Relat. Fields*, 16:549–598, 2010.

[9] N. Berglund and B. Gentz. Sharp estimates for metastable lifetimes in parabolic SPDEs: Kramers' law and beyond. *Electron. J. Probab.*, 18:no. 24, 58, 2013.

[10] A. Bovier, M. Eckhoff, V. Gayrard, and M. Klein. Metastability in reversible diffusion processes. I. Sharp asymptotics for capacities and exit times. *J. Eur. Math. Soc. (JEMS)*, 6(4):399–424, 2004.

[11] A. Bovier, V. Gayrard, and M. Klein. Metastability in reversible diffusion processes. II. Precise asymptotics for small eigenvalues. *J. Eur. Math. Soc. (JEMS)*, 7(1):69–99, 2005.

[12] M. Cameron and E. Vanden-Eijnden. Flows in complex networks: theory, algorithms, and application to Lennard-Jones cluster rearrangement. *J. Stat. Phys.*, 156(3):427–454, 2014.

[13] A. S. Deif. Rigorous perturbation bounds for eigenvalues and eigenvectors of a matrix. *J. Comput. Appl. Math.*, 57(3):403–412, 1995.

[14] F. den Hollander. Metastability under stochastic dynamics. *Stochastic Process. Appl.*, 114(1):1–26, 2004.

[15] F. den Hollander and S. Jansen. Metastability at low temperature for continuum interacting particle systems. In preparation.

[16] S. Dutercq. In preparation. 2015.

[17] S. Dutercq. *Métastabilité dans les systèmes avec loi de conservation*. PhD thesis, Université d'Orléans, 2015.

[18] H. Eyring. The activated complex in chemical reactions. *Journal of Chemical Physics*, 3:107–115, 1935.

[19] L. Flatley and F. Theil. Face-centered cubic crystallization of atomistic configurations. *Archive for Rational Mechanics and Analysis*, 218(1):363–416, 2015.

[20] M. I. Freidlin and A. D. Wentzell. *Random Perturbations of Dynamical Systems*. Springer-Verlag, New York, second edition, 1998.

[21] G. H. Golub and C. F. Van Loan. *Matrix computations*. Johns Hopkins Studies in the Mathematical Sciences. Johns Hopkins University Press, Baltimore, MD, fourth edition, 2013.

[22] K. Hun. Metastability in interacting nonlinear stochastic differential equations. Master's thesis, Université d'Orléans, 2009.

[23] S. Jansen and P. Jung. Wigner crystallization in the quantum 1D jellium at all densities. *Comm. Math. Phys.*, 331(3):1133–1154, 2014.

[24] J. P. Keener. Propagation and its failure in coupled systems of discrete excitable cells. *SIAM J. Appl. Math.*, 47(3):556–572, 1987.

[25] H. A. Kramers. Brownian motion in a field of force and the diffusion model of chemical reactions. *Physica*, 7:284–304, 1940.

[26] J.-C. Mourrat and H. Weber. Convergence of the two-dimensional dynamic Ising-Kac model to Φ^4_2. Preprint `arXiv:1410.1179`, 2014.

[27] E. Olivieri and M. E. Vares. *Large deviations and metastability*, volume 100 of *Encyclopedia of Mathematics and its Applications*. Cambridge University Press, Cambridge, 2005.

[28] F. Otto, H. Weber, and M. G. Westdickenberg. Invariant measure of the stochastic Allen-Cahn equation: the regime of small noise and large system size. *Electron. J. Probab.*, 19:no. 23, 76, 2014.

[29] J. Rubinstein and P. Sternberg. Nonlocal reaction-diffusion equations and nucleation. *IMA J. Appl. Math.*, 48(3):249–264, 1992.

[30] J.-P. Serre. *Linear representations of finite groups*. Springer-Verlag, New York, 1977. Translated from the second French edition by Leonard L. Scott, Graduate Texts in Mathematics, Vol. 42.

[31] E. Vanden-Eijnden and M. G. Westdickenberg. Rare events in stochastic partial differential equations on large spatial domains. *J. Stat. Phys.*, 131(6):1023–1038, 2008.

Contents

Université d'Orléans, Laboratoire Mapmo
CNRS, UMR 7349
Fédération Denis Poisson, FR 2964
Bâtiment de Mathématiques, B.P. 6759
45067 Orléans Cedex 2, France
E-mail addresses: nils.berglund@univ-orleans.fr, sebastien.dutercq@univ-orleans.fr